

Viscosity as a Smoking Gun for Complex Formation in Solution: Fe^{2+} and Mg^{2+} Chlorides as Examples

Amrita Goswami,[†] Samuel Blazquez,[‡] Lucía Fernández-Sedano Vázquez,[‡] Eva González Noya,[¶] Hannes Jónsson,[†] Jacobo Troncoso,[§] and Carlos Vega^{*,‡}

[†]*Science Institute and Faculty of Physical Sciences, University of Iceland, VR-III, 107 Reykjavík, Iceland*

[‡]*Departamento de Química Física, Facultad de Ciencias Químicas, Universidad Complutense de Madrid, 28040 Madrid, Spain.*

[¶]*Instituto de Química Física Blas Cabrera, CSIC, C/Serrano 119, 28006 Madrid, Spain.*

[§]*Departamento de Física Aplicada, Universidade de Vigo, Escola de Enxeñaría Aeronáutica e do Espazo, E 32004, Ourense, Spain*

E-mail: cvega@ucm.es

Abstract

Electrolyte solutions at high concentration are indispensable and yet poorly understood. In particular, the extent of speciation – the formation of complexes composed of multiple species – in concentrated ionic solutions is very challenging to obtain theoretically and experimentally, but can have a strong effect on solution properties. The literature is rife with contradictory estimates of speciation from experiments. We find that speciation affects transport properties, and is therefore, a prerequisite to accurately model concentrated solutions. We turn this to our advantage by showing that the viscosity can be used to determine the extent of complexation in concentrated aqueous solutions. Results of simulations as well as experimental measurements are presented. The atomistic Madrid-2019 force-field is extended to model FeCl_2 . Solutions of FeCl_2 and MgCl_2 are compared and the observed difference in viscosity explained by more complexation in the former, a conclusion supported by recently reported X-ray absorption and neutron scattering experiments.

1 Introduction

Electrolytes in water are omnipresent in nature and play a vital role in practical and industrial applications.^{1–4} For example, seawater is an electrolyte solution,⁵ and many of the ions that are abundant in the sea are also present in living cells.⁶ Given the ubiquity and relevance of electrolyte solutions, it is perhaps surprising that a rigorous and practical theory for electrolytes at high concentration is not available. Many successful theories, such as the elegant Debye–Hückel theory,⁷ approach electrolyte solutions from the infinitely dilute limit, and thus, quite intuitively, work only for dilute solutions.⁸ The behaviour of electrolyte solutions at high concentration is difficult to extrapolate from this infinitely dilute limit because of effects such as complex formation, ion pairing, etc., which cannot be easily shoehorned into a single mathematical framework.

The extent to which ions of opposite charge form long-lived ion pairs is, therefore, an important and divisive issue. The existence of complexes can significantly affect various properties of electrolyte solutions, particularly so at high concentration.⁹ However, experimental estimates differ

widely on the extent of complexation, as well as on the equilibrium distribution of different types of complexes. For example, values reported in the literature for the equilibrium constant, $\log K$, of FeCl^+ formation in aqueous FeCl_2 solution, range from 0.74^{10} to -0.89^{11} with multiple values in between.^{12–17} Various measurements at 4 m have, in particular, yielded contradictory results. The spectrophotometric experiments of Zhao and Pan¹⁷ suggest that the monochloro complex $[\text{FeCl}(\text{H}_2\text{O})_5]^+$ is the predominant species in solution, with a small amount of the neutral trans dichloro complex $[\text{FeCl}_2(\text{H}_2\text{O})_4]$. However, X-ray absorption spectroscopy measurements of Luin et al.¹⁸ provide evidence for the conclusion that the neutral trans dichloro complex $[\text{FeCl}_2(\text{H}_2\text{O})_4]$ is the dominant species. In contrast, THz/FIR absorption spectra of Böhm et al.¹¹ indicate the presence of only the monochloro complex.

Chemical equilibrium models can predict speciation using activity models, for example Specific Ion Theory (SIT)^{19–21} and the Davies equation,²² using ion association constants (typically obtained from experiments).^{13,23} However, the quality of the results depends strongly on (i) the activity model used, which may fail at high concentration, and (ii) the accuracy of the ion association constants. Discrepancies can arise due to inherent differences in experimental measurement methods. For instance, an equilibrium constant calculated using the anion exchange method,²⁴ which is sensitive only to contact ion pairs, can be smaller than one estimated using potentiometry.²⁵

Atomic-scale simulations using empirical potential functions can only approximately describe the interaction between molecules and ions. Despite this, they can still be used to learn some physics about electrolytes, thus extending our understanding of ionic solutions (at least qualitatively) beyond the Debye-Hückel limit. However, predicting both the dynamics of complex formation and the equilibrium distribution of complexes accurately can be challenging with simple point charge models.²⁶

Density functional theory (DFT) has been successfully used to describe interactions between cations, water and anions in ionic solutions.^{27–29} However, although quantum mechanical calculations can provide insight into the stability of spe-

cific complexes, they are infeasible to determine the equilibrium distribution of complexes due to their high computational costs and limited system size.

Therefore, the degree of complexation is difficult to ascertain from experiments, simulations and theory. On the other hand, as discussed above, knowledge of complexation and complex distributions is crucial, since they can strongly affect solution properties. Here, we demonstrate that this problem can be turned on its head: viscosity can instead be used as a guide to infer the extent of complexation.

We accomplish this by performing both experiments, for FeCl_2 , and simulations, comparing FeCl_2 and MgCl_2 . In order to describe FeCl_2 in simulations, we extend the Madrid-2019 force-field³⁰, which is a simple empirical force-field wherein monoatomic ions are represented by single Lennard-Jones (LJ) centers with a scaled charge. We include complexes in our simulations by freezing distances between cation-chloride ion pairs. By explicitly including a fixed number of monochloro and dichloro complexes, and varying these constant proportions over a number of simulation trajectories, we show that the effect on the viscosity is surprisingly large and measurable. We present clear evidence of higher association in FeCl_2 , compared to MgCl_2 . This in contrast with the equilibrium values for association recommended by NIST,³¹ but which is in line with more recent experimental measurements.^{18,32}

2 Methods

2.1 Experimental

Ferrous chloride was purchased from Sigma-Aldrich, with a purity greater than 0.99 in mass fraction. MilliQ water was used to prepare the solutions, made by weight in an AE-240 Mettler Toledo balance, with an uncertainty of 0.1 mg, and in an atmosphere of N_2 to avoid Fe^{2+} oxidation. Uncertainty in concentration is estimated to be 0.004 mol/kg. Densities were measured using a DMA5000 vibrating tube densimeter from Anton Paar. Since the densities of the investigated solutions reach high values, calibration was performed

using MilliQ water and carbon tetrachloroethylene, purchased from Sigma Aldrich with a purity greater than 0.999 in mass fraction. The viscosity of the solutions is small enough to neglect any correction due to damping of the vibrating tube oscillations. Uncertainty in density is estimated to be 0.0003 g/cm^3 . More details about the procedure for density measurements can be found elsewhere.³³ Viscosities were measured using an AMVn falling ball viscometer, calibrated using MilliQ water, details of which are present in the literature.³⁴ Relative uncertainty in this magnitude is estimated to be 2%. The experimental technique was validated by reproducing experimental densities and viscosities of MgCl_2 from previous work.^{35,36} The density and viscosity were determined for fourteen solutions at 298.15 K, in the concentration interval (0-4.1) mol/kg.

2.2 Computational

Table 1: Force-field parameters for the Fe^{2+} and Cl^- ions. The values for $q = 0.85 e$ are those of the Madrid-2019 force field for Mg^{2+} . The parameters which are different in the $q = 0.80 e$ model, compared to the original model with $q = 0.85 e$, are highlighted in bold text.

$q = 0.85 e$		
	σ_{ij} (nm)	ϵ_{ij} (kJ/mol)
$\text{Fe}^{2+} - \text{Fe}^{2+}$	0.116290	3.651900
$\text{Fe}^{2+} - \text{Cl}^-$	0.300000	3.000000
$\text{Fe}^{2+} - \text{O}_w$	0.181000	12.00000
$\text{Cl}^- - \text{Cl}^-$	0.469906	0.076923
$\text{Cl}^- - \text{O}_w$	0.423867	0.061983
$q = 0.80 e$		
	σ_{ij} (nm)	ϵ_{ij} (kJ/mol)
$\text{Fe}^{2+} - \text{Fe}^{2+}$	0.116290	3.651900
$\text{Fe}^{2+} - \text{Cl}^-$	0.300000	3.000000
$\text{Fe}^{2+} - \text{O}_w$	0.185000	12.00000
$\text{Cl}^- - \text{Cl}^-$	0.469906	0.076923
$\text{Cl}^- - \text{O}_w$	0.418801	0.061983

Molecular Dynamics (MD) simulations were performed using both GROMACS (version 2025.2)³⁷ and LAMMPS (29 Aug 2024, Update 1)³⁸; see Sec. 1.1.1 and Sec. 1.1.2 in the SI for details. All results were obtained at ambient conditions (i.e., 298.15 K and 1 bar). Atomic-scale simulations have been performed using the Madrid-2019 force-field,³⁰ which combines the TIP4P/2005 model of water³⁹ and scaled charges for the ions, such that monoatomic cations have a charge of $q = 0.85 e$. The use of scaled charges (also denoted as the Electronic Continuum Correction) is becoming a popular strategy in the literature.^{8,40-46}

A version of the force-field with a charge of $0.80 e$ has also been used in this work. Parameters for Mg^{2+} (for $q = 0.85 e$) and Cl^- (for both $q = 0.85 e$ and $q = 0.80 e$) have been reported previously^{30,47} whereas the parameters for Mg^{2+} (for $q = 0.80 e$) were obtained in this work. The proposed force-field parameters for Fe^{2+} and Cl^- are presented in Table 1. These parameters are the same as those of Mg^{2+} .³⁰ Justifications for using the same force-field are provided in Sec. 3.2.1. Naturally, the correct masses should be used for Fe^{2+} and Mg^{2+} .

The molality scale, m , has been used for concentrations.

3 Results

3.1 Measured density and viscosity of FeCl_2

Table 2: Experimentally measured density and viscosity of FeCl_2 at various concentrations.

Molality (mol/kg)	Density (g/cm^3)	η (mPa·s)
1.000	1.10188	1.286
2.000	1.19758	1.846
3.000	1.28578	2.663
4.000	1.36809	4.170

Although the solubility limit of FeCl_2 is about 5.5 m at room temperature and ambient pressure,⁴⁸ the literature lacks values for the density and viscosity for concentrations above 2 m³⁵ and

0.4 m,³⁶ respectively. Data is reported here for up to 4 m. Interpolated values at round numbers for the density and viscosity are provided in Table 2. Good agreement is found with existing literature values for the more dilute solutions [see also Fig. S2(a) in the SI].^{35,36}

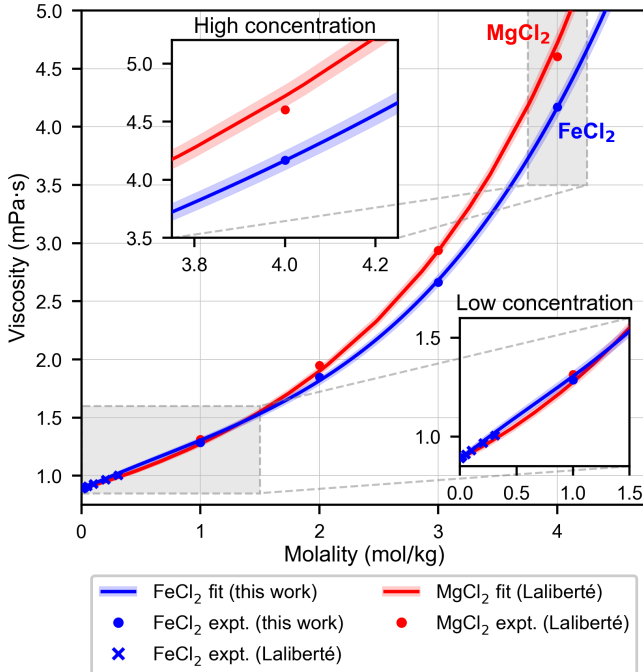


Figure 1: Viscosity of FeCl_2 and MgCl_2 from experiments, obtained from Laliberté³⁶ and this work. The blue shaded region corresponds to a 2% relative uncertainty in the FeCl_2 viscosity measurements reported in this work. The red shaded region represents the 1.8% mean relative deviation of the Laliberté model for MgCl_2 from the experimental data³⁶. Inset, bottom: Zoomed-in view of viscosities at low concentration, which are similar in value. Inset, top: Close-up view of the stark difference between the experimental viscosity of FeCl_2 and MgCl_2 at high concentration.

Fig. 1 shows the experimental viscosities of FeCl_2 and MgCl_2 at both low and high concentration. For concentrations less than 2 m, the viscosities are similar, within errors (lower inset in Fig. 1). The viscosity of electrolyte solutions is often described by the Jones-Dole equation:⁴⁹

$$\eta/\eta_w = 1 + A\sqrt{m} + Bm + Cm^2 \quad (1)$$

where η is the viscosity of the aqueous solution, η_w is the viscosity of water, m is the mo-

lality, the term A [which is small⁵⁰ and around $0.02 \text{ (kg/mol)}^{1/2}$ for MgCl_2 and FeCl_2] describes charge-charge contributions in the highly diluted region. The B coefficient (in units of kg/mol) is characteristic of individual ions, is additive, and can be interpreted in terms of ion-water interactions.⁵¹ The term C [in units of $(\text{kg/mol})^2$] is thought to depend on solute-solute association effects.⁵²

Typically in experiments, the Jones-Dole coefficient B is obtained by fitting the viscosity at low concentrations (i.e., below 0.6 m), where the quadratic term can be safely neglected. As can be expected from the similar viscosities of FeCl_2 and MgCl_2 at low concentration, the experimental values of B for FeCl_2 and MgCl_2 are almost identical, equal to $0.405(10) \text{ kg/mol}$ and $0.375(10) \text{ kg/mol}$, respectively (see also Sec. 3.2.2 for a comparison with simulations).⁴⁹ The value of B for FeCl_2 is slightly higher than that of MgCl_2 , which could account for the corresponding marginally higher viscosity of the former compared to the latter at low concentration.

However, the experimental viscosities of FeCl_2 and MgCl_2 , at high concentration, differ significantly, which is highlighted in the top inset of Fig. 1. Eq. (1) describes the viscosities well up to a concentration of 3 m. We have estimated the values of C as 0.12 (kg/mol)^2 and 0.08 (kg/mol)^2 for MgCl_2 and FeCl_2 , respectively, by fitting the experimental viscosities up to 3 m. At higher concentrations, a cubic D term [with units of $(\text{kg/mol})^3$] would have to be added to Eq. (1) to reproduce the experimental viscosities.

The existence of monochloro and dichloro complexes in FeCl_2 has been reported at concentrations around 4 m.^{11,17,18} On the other hand, MgCl_2 being a strong 2:1 electrolyte, reportedly shows little or no complexation even at higher concentrations.^{26,53,54} In subsequent sections, we provide evidence from simulations that suggests that the difference of Fe^{2+} and Mg^{2+} in their propensity to complexation is tied to differences in their viscosity at high concentration, as already suggested by the large difference in the value of C (33%) between both systems.

3.2 Simulations without complexes

3.2.1 A force-field for FeCl₂

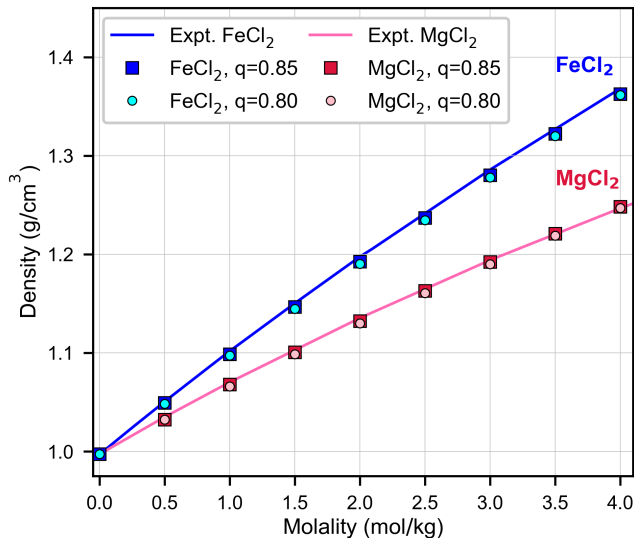


Figure 2: Density of FeCl₂ and MgCl₂ from fits to experiments (solid blue and magenta line, respectively) from this work and Laliberté and Cooper³⁵, Laliberté³⁶, respectively, as well as the density from atomic-scale simulations without complexes (squares and circles). Agreement is within 0.5% for all concentrations.

Fig. 2 presents a comparison of experimental densities with those obtained from simulations, using the same force-field for MgCl₂ and FeCl₂, at various concentrations. Agreement between simulations and experiments is within 0.5% for both the 0.85 and 0.8 charge models. Solution densities are often used as target properties in parameterization,^{30,55} and consequently, the good agreement with experiments at low and high concentration validates the approximation of using Mg²⁺ force-field parameters for Fe²⁺.

When the same force-field is used for FeCl₂ and MgCl₂, an inherent assumption is that the number densities of both solutions are the same and that, consequently, the following relation holds true:

$$\rho_{\text{FeCl}_2} = \rho_{\text{MgCl}_2} \frac{1000 + m \times M_{\text{FeCl}_2}}{1000 + m \times M_{\text{MgCl}_2}}, \quad (2)$$

where ρ_{MgCl_2} and ρ_{FeCl_2} are the mass densities in g/cm³, M_{MgCl_2} and M_{FeCl_2} are the molar masses

in g/mol of MgCl₂ and FeCl₂, respectively, and m is the molality of the solutions in mol/kg.

At low concentration, the assumption of equal number densities is a reasonable one, since the experimental values of the cation-oxygen distance and the hydration free energy of Fe²⁺ and Mg²⁺ are quite similar (collected in Table S1 in the SI). In order to evaluate whether this assumption is also valid at higher concentrations, we estimated the mass density of FeCl₂, using Eq. (2), from experimental MgCl₂ densities, and compared the former with corresponding experimental densities, obtaining good agreement, as shown in Fig. S2(a) in the SI. This simple test is also passed for Fe(SO₄) and Mg(SO₄), as shown in Fig. S2(b) in the SI. More generally, we believe that Eq. (2) can be used to easily test whether the force-field parameters of one cation can be reasonably used for another target cation (at least for density predictions) since such an evaluation would only require experimental densities at different concentrations.

3.2.2 Transport properties of solutions without complexes

The experimental data obtained for FeCl₂ enables us to examine trends in the viscosity at high concentration, where the effect of complexes is expected to be important. However, complexes do not form spontaneously in our atomic-scale simulations of FeCl₂ and MgCl₂. This is because obtaining the equilibrium complex population would require much longer simulation time, on the order of microseconds, since this is the experimental residence time of water^{56,57} in solvation shells of Mg²⁺ or Fe²⁺.

Fig. 3 shows the experimental values for the viscosity of FeCl₂ and MgCl₂, along with results obtained from simulations (red and blue squares). At concentrations below 2 m, the viscosity of MgCl₂ and FeCl₂ obtained from simulations agree with experiments well, and this is also the regime where the experimental viscosities are quite similar (lower inset in Fig. 1).

Furthermore, at a concentration of 0.6 m, it can be assumed that the quadratic term in Eq. (1) is negligible (elaborated in Sec. S12 in the SI). We estimated B coefficients for the 0.80 Madrid-2019 model by determining the viscosity at this concen-

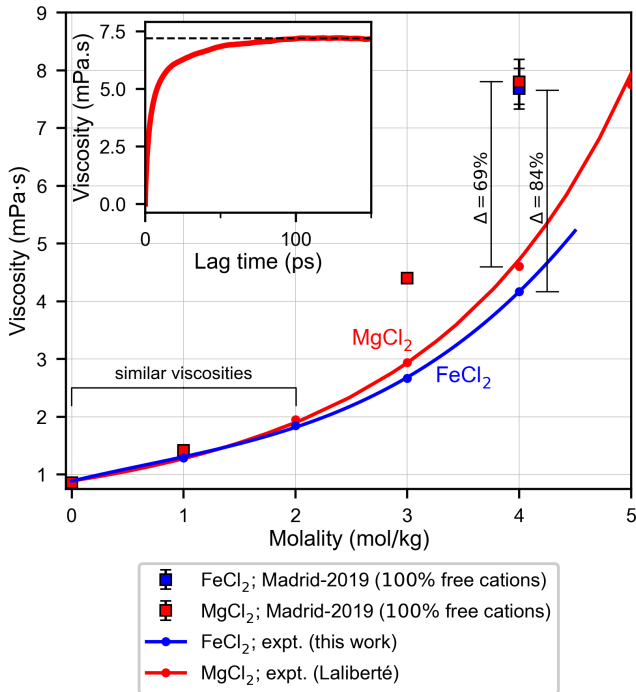


Figure 3: Comparison of the viscosity of FeCl_2 and MgCl_2 obtained from simulations using the Madrid-2019 model (blue and red squares) with those from experiments (solid blue and red line, respectively). Inset: The viscosity obtained from the Green-Kubo formalism for a 4 m MgCl_2 solution, showing that the viscosity plateaus at about 100 ps at the converged value.

Table 3: Jones-Dole B coefficients from simulations (B_{sim}), computed using the 0.80 Madrid-2019 model, and those from experiments (B_{expt}) for FeCl_2 and MgCl_2 .

System	B_{sim} (kg/mol)	B_{expt} (kg/mol)
FeCl_2	0.46(3)	0.405(10) ^a
MgCl_2	0.42(3)	0.375(10) ^a

* a) From Marcus⁴⁹

tration (see also Sec. S12 in the SI for details of these calculations). Table 3 presents these values, which are about 0.04 kg/mol higher than experimental values. Given that non-polarizable models with unscaled charges are known to overestimate B by approximately 0.16 kg mol^{-1} for 1:1 electrolytes⁵⁸, with even larger deviations expected for 2:1 electrolytes, the level of agreement observed here is very good.

On the other hand, Fig. 3 shows that results from

simulations deviate significantly from experiments at high concentrations around 4 m. The trends in Fig. 3 seem to suggest that the microstructure of FeCl_2 and MgCl_2 solutions is inherently different at high concentration, and that simulations which do not account for this fail to describe such solutions.

3.3 Simulations with complexes

As touched upon previously in Sec. 3.2.2, the formation of complexes is not observed even after 200 ns runs with the Madrid-2019 force-field. Additional interactions would need to be included to capture complex formation.²⁶ We conclude that both the long timescale for attaining the equilibrium complex distribution in concentrated solutions, and the challenge of describing the interaction between the ions at such close range, make simulations describing the dynamics of complex formation impractical at this time (see Sec. 4.3 for an expanded discussion).

Here, we make a distinction between the somewhat synonymous terms – contact ion pairs (CIPs) and complexes – used in the literature. We use the term CIP when the residence time of the anion in contact with the cation is relatively low (from a few to dozens of picoseconds), such as in the case of NaCl .⁵⁹ We assume that the lifetime of such CIPs is less than the typical decay time of the stress autocorrelation function for the solution (which is around 100-200 ps for the systems considered in this work as shown in the inset of Fig. 3). In this work, we use the term complex when the residence time of the anion in contact with the cation is significantly larger than the decay time of the stress autocorrelation function, so that we can assume that their distribution does not change significantly during the course of a simulation trajectory used to calculate physical quantities of interest (here, the viscosity and diffusion coefficient).

3.3.1 A simulation strategy for including complexes

In our simulations, we model complexes by freezing the cation-chloride distance to 2.33 \AA (see Sec. 4 of the SI for justifications) Concomitantly, water molecules are allowed to move, and are free

to translate, rotate, and even leave the solvation shell. Freezing the cation-anion distances is a reasonable approximation, since cation-chloride vibrations within the complex are not expected to have a significant effect on the viscosity or diffusion coefficient.

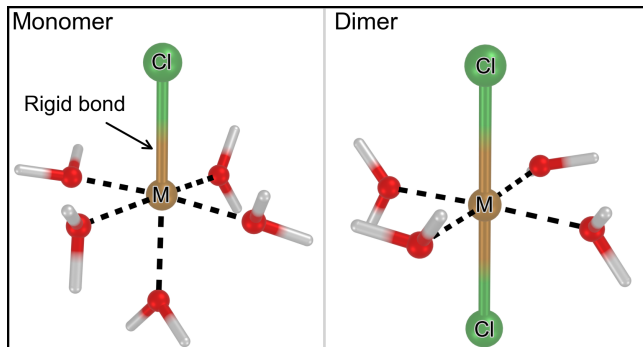


Figure 4: Illustration of the complexes considered in the atomic-scale simulations. The bond between the metal cation and Cl^- anion is rigid, but the water molecules are free to move. The black dashed lines indicate the octahedral shape of the solvation shell. *Left*: The *monomer* complex, wherein the cation is part of a monochloro complex (where M corresponds to an Fe^{2+} or Mg^{2+} cation). *Right*: The *dimer* complex, consisting of a linear dichloro unit $\text{Cl}-\text{M}-\text{Cl}$.

Complexes can also exhibit a plethora of structures, which is why speciation generally refers to a distribution of these types. We use the following terminology to describe two of the most dominant types of complexes formed by Fe^{2+} ^{11,17,18} and Mg^{2+} ,^{54,60} illustrated in Fig. 4. A *monomer* (Fig. 4 left) refers to a complex formed by one cation, coordinated with one Cl^- anion and some additional molecules of water in the first solvation shell, with the cation-chloride distance frozen. A *dimer* (Fig. 4 right) refers to a complex wherein there are two Cl^- anions in the trans position of the octahedron, along with additional coordinating water molecules.

In our new simulation strategy, instead of attempting to model the dynamics of complex formation, we *introduce a fixed number of complexes* (monomers and/or dimers) at the beginning of simulations as an input and constrain the cation-chloride distance in the complex to study the effect that complex distributions can have on the properties of the solutions.

This strategy was validated by analyzing the structures of the solvation shell around free cations, monomers and dimers. The octahedral solvation structure was retained by monomers and dimers, showing that constraining the cation-chloride distance does not distort the solvation shell around the cation (Fig. S3 in the SI).

In addition, the effect of complexes on the density is small, at least when considering only octahedral complexes (see Table S3 in SI; the density increases by only 0.5% at 4 m when all cations participate in monomers and there are no free cations). Therefore, the introduction of monomers and dimers does not cause the excellent density predictions of the force-field to deteriorate.

3.3.2 The effect of complexes on transport properties

We denote α as the percentage of free cations, α' as the percentage of monomers and α'' as the percentage of dimers, such that:

$$\alpha + \alpha' + \alpha'' = 100. \quad (3)$$

First, we analyze the impact of monomers (illustrated in Fig. 4) on the viscosity. When considering only free ions and monomers, α'' is zero. We vary the fraction of free cations, α , from 100% (where all ions are free) to 0% (where all cations form monomers).

Table 4: Viscosity (in mPa·s) of FeCl_2 and MgCl_2 solutions at 4 m obtained from simulations using the Madrid-2019 force field. The Yeh-Hummer correction⁶¹ was used to account for finite-size effects.

System	α	$D_{\text{H}_2\text{O}} \times 10^9$ (m ² /s)	η (mPa·s)
MgCl_2	100	0.366	7.73(0.39)
MgCl_2	15	0.499	5.71(0.33)
MgCl_2	2.5	0.522	5.56(0.42)
FeCl_2	100	0.369	7.68(0.41)
FeCl_2	15	0.496	5.87(0.30)
FeCl_2	2.5	0.522	5.54(0.32)

The viscosity and diffusion coefficient of water obtained in simulations for 4 m solutions of FeCl_2 and MgCl_2 are presented in Table 4. Fig. 5

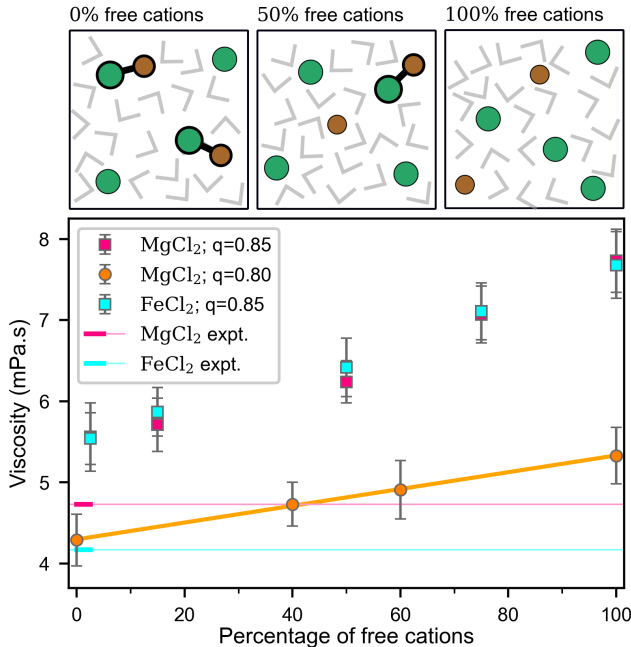


Figure 5: The experimentally measured viscosity of a 4 m solution of MgCl_2 ³⁶ and FeCl_2 depicted as magenta and cyan horizontal lines, respectively, as well as the calculated viscosity (squares) of solutions containing a varying fraction of monomer complexes and free ions, shown as a function of the percentage of free cations, α . The orange circles depict calculated viscosity of MgCl_2 using the Madrid-2019 force-field with a charge of $0.80 e$. Insets on top illustrate solutions with no free cations, 50% free cations and only free cations.

shows the viscosities of MgCl_2 and FeCl_2 at 4 m (at 298.15 K and 1 bar), for different complex distributions (i.e., different proportions of free cations and monomers). The experimental viscosities of MgCl_2 and FeCl_2 at this concentration are also depicted. We observe that the viscosities of FeCl_2 and MgCl_2 from simulations are roughly the same (within our uncertainty, which is 0.25-0.45 mPa.s). Notably, the presence of complexes (monomers, in this case) significantly reduces the value of the viscosity – the viscosity of MgCl_2 goes from ≈ 7.73 mPa.s when $\alpha = 100$ to ≈ 5.5 mPa.s when $\alpha = 0$. Note that this last value of the viscosity, 5.5 mPa.s, is closer to the experimental result (4.73 mPa.s).³⁶

The explanation of the decrease of viscosity with increase in complexes is intuitive: water molecules in the vicinity of ions diffuse more slowly than wa-

ter molecules in the bulk.⁶² Additionally, the net charge of a monomer is half of that of a free cation, thereby exerting a weaker electric field on the surrounding water molecules. Thus, the presence of complexes (monomers, in this case) reduces the net amount of encumbered water molecules in contact with the ions, compared to solutions with free ions.

Consequently, the diffusion of water increases with a rise in the number of complexes, as shown in Table 4. The observation that the viscosity and the diffusion coefficient of water are anti-correlated in electrolyte solutions was discussed and shown by McCall and Douglass⁶³ more than sixty years ago. This suggests that experimental measurements of $D_{\text{H}_2\text{O}}$ could also serve as an indirect measure of complex formation in these systems.

However, even after introducing monomers, quantitative agreement with experiments is not achieved. Fig. 5 shows that even if we assume 100% population of monomers and no free cations, neither the viscosity of MgCl_2 nor that of FeCl_2 is reproduced. Of course, one should not disregard the presence of other complexes in the system, for instance those formed by the FeCl_2 species (or the dimer species, in our terminology, see Fig. 4).

Since dimers presumably hinder even less water molecules than monomers, we surmise that the presence of dimers should reduce the viscosity further. At 4 m with $\alpha'' = 100$ (all the cations form dimers), the viscosity of the system (either MgCl_2 or FeCl_2) is calculated to be 4.8(0.2) mPa.s, which is lower than that of the system wherein all complexes form monomers [≈ 5.5 mPa.s]. However, this reduction is still not low enough to reach the experimental viscosity of FeCl_2 , which is 4.17 mPa.s (as shown in Table 2).

We also analyze the results of simulations with the 0.8 Madrid-2019 model, which tends to improve the description of transport properties, compared to the 0.85 model.^{64,65} Using this model, it is possible to reproduce the experimental viscosity of both MgCl_2 and FeCl_2 , by assuming 40% of free cations for MgCl_2 and 0% for FeCl_2 (i.e., all cations participate in monomers), as shown in Fig. 5 (Table S7 in the SI presents simulation results with 100% dimers). Our results indicate a

35–40% greater degree of complex formation in FeCl₂ compared to MgCl₂. Therefore, we surmise that the association for FeCl₂ is significantly more important than for MgCl₂, a conclusion supported by recent experiments.^{18,32}

4 Discussion

4.1 Complex populations: the thermodynamic formalism

Although experiments of FeCl₂ solutions unanimously report the existence of complexes at high concentration, there is little consensus on the nature and type of dominant complexes formed.^{11,17,18} We speculate that determining their precise equilibrium distribution can be quite difficult from experiments, and, to the best of our knowledge, quantitative complex distributions have not been reported so far.

Another conceptually attractive route to estimating complex populations could be to obtain equilibrium constants. We define the equilibrium constant K_1 for the reaction $M^{2+} + Cl^- \rightleftharpoons MCl^+$ as:

$$K_1 = \frac{a_{MCl^+}}{a_{M^{2+}} a_{Cl^-}} = \frac{[MCl^+]}{[M^{2+}][Cl^-]} \frac{\gamma_{MCl^+}}{\gamma_{M^{2+}} \gamma_{Cl^-}}, \quad (4)$$

where M refers to the metals considered here (Fe or Mg), a_i is the activity of component i , and γ_i is its activity coefficient, and $[i]$ is the concentration of component i .

However, there is a wide disparity in the value of the estimated equilibrium constant K_1 . Table 5 presents $\log K_1$ from the literature, which varies from 0.74 to -0.89 for FeCl₂, corresponding to a difference of almost two orders of magnitude. The value of $\log K_1$ of FeCl₂ recommended by NIST is -0.2 , which lies squarely in the middle of the range shown in Table 5. The same is true for MgCl₂, although it has been studied much less than FeCl₂,^{13,23} and the general consensus is that MgCl₂ has low propensity to form complexes.^{26,53,54}

However, quantifying complex populations involves another contentious issue: activities (for instance, a_{MCl^+} , $a_{M^{2+}}$, a_{Cl^-}), and not concentrations, need to be estimated for real solutions. Individual

Table 5: Equilibrium constants $\log(K_1)$ for monomer formation of the reaction $M^{2+} + Cl^- \rightleftharpoons MCl^+$, where M refers to the metal.

FeCl ₂	
H. Olerup (1944) ¹²	0.36
Wells and Salam (1967) ¹⁰	0.74
Arnorsson et al.(1982) ¹³	-0.40
J.R.Ruaya (1988) ¹⁴	-0.50
Heinrich and Seward (1990) ¹⁵	-0.16
Palmer and Hyde (1993) ¹⁶	-0.125
Zhao and Pan (2001) ¹⁷	-0.366
Böhm et al. (2015) ¹¹	-0.89
NIST	-0.2
MgCl ₂	
J.R.Ruaya (1988) ¹⁴	-0.13
NIST	0.6

activity coefficients cannot be directly calculated from experiments. Activity models, such as Specific Ion Theory (SIT)^{19–21} or the Davies equation²² are often used to estimate complex populations, given equilibrium constant values. Chemical equilibrium models, such as Visual MINTEQ (version 4.0),²³ can estimate percentage distributions of free cations, using such activity models. However, even when starting from the same equilibrium constant (for instance, those recommended by NIST), different activity models yield widely diverging complex populations, as shown in Table 6.

Table 6: Percentage of free cations, α , in 4 m aqueous solutions at room temperature and pressure, obtained from Visual MINTEQ²³ using different activity models and association constants from NIST. The column labeled $\gamma = 1$ refers to results obtained from Eq. (4) using the approximation that all activity coefficients are unity. More association is predicted for MgCl₂ than for FeCl₂.

System	Activity model		
	SIT	Davies	$\gamma = 1$
MgCl ₂	8%	0.5%	6%
FeCl ₂	29%	3%	24%

As can be expected, calculations using such chemical equilibrium models are sensitive to the quality of the activity model and the ion association constants. We surmise that, at this point, they are not reliable enough to unambiguously determine the concentration of complexes.

4.2 Toy model exploiting the relationship between complex populations and viscosity

In Sec. 3.3.2, we presented a model that could reproduce the experimental viscosities of FeCl₂ and MgCl₂ simultaneously, contingent on a particular (variable) complex population used to fit to the viscosity (solid orange line in Fig. 5).

Simulation results notwithstanding, we cannot claim to quantitatively determine the equilibrium concentration and the type of complexes that actually exist experimentally in FeCl₂ and MgCl₂. However, we will try to develop a toy model that, although approximate, can at least qualitatively describe the high concentration viscosity trends of FeCl₂ and MgCl₂.

We introduce a second equilibrium constant, K_2 , defined as the equilibrium constant for the reaction $\text{MCl}^+ + \text{Cl}^- \rightleftharpoons \text{MCl}_2^0$ according to:

$$K_2 = \frac{a_{\text{MCl}_2^0}}{a_{\text{MCl}^+} a_{\text{Cl}^-}} = \frac{[\text{MCl}_2^0]}{[\text{MCl}^+][\text{Cl}^-]} \frac{\gamma_{\text{MCl}_2^0}}{\gamma_{\text{MCl}^+} \gamma_{\text{Cl}^-}}, \quad (5)$$

where symbols have the same meaning as in Eq. (4).

In addition to relations for the equilibrium constants, we need a model to describe how the viscosity changes as the population of complexes changes. We propose a simple and heuristic approach, and suggest the following equation to estimate the viscosity at 4 m for MgCl₂ and FeCl₂

$$\eta(4 \text{ m}) = \eta^0 - \delta' \alpha' - \delta'' \alpha'' \quad (6)$$

where η^0 is the viscosity (in mPa·s) of a solution with 100% free cations.

The basis for this formula is the observation that the viscosity changes linearly with the number of monomers, in the absence of dimers, and also that the viscosity changes linearly (albeit with a different slope) with the number of dimers, in the

absence of monomers. The value of the slopes, can be obtained from the simulations of this work. We obtain values of $\delta'_{q=0.85 e} = 0.020$ mPa·s and $\delta'_{q=0.80 e} = 0.010$ mPa·s for the $q = 0.85 e$ and $q = 0.80 e$ models, respectively, from the slopes in Fig. 5. For δ'' , we obtain $\delta''_{q=0.85 e} = 0.029$ mPa·s and $\delta''_{q=0.8 e} = 0.014$ mPa·s (derived in Sec. 11 in the SI).

Secondly, we need the values of the association constants K_1 and K_2 . We shall use the NIST value for K_1 of FeCl₂ [i.e., $\log(K_1) = -0.20$]. However, obtaining a value for K_2 is more cumbersome. As shown in Sec. 11 of the SI, $\log K_2$ is often around 0.8 units smaller than $\log K_1$ (see also Table 6.1 in Burgess⁵⁷). Therefore, we adopt the values of $\log K_2$ for FeCl₂ and MgCl₂ listed in Table 7. Note that we imposed a smaller value of K_1 for MgCl₂, compared to that of FeCl₂. This was motivated by the observation that MgCl₂ is an archetypal strong 2:1 electrolyte that exhibits little complexation in concentrated solutions.⁵⁴

Table 7: Values of equilibrium constants* used for a qualitative calculation of the viscosity of FeCl₂ and MgCl₂ at 4 m, estimated complex distributions (exemplified by α , α' , α''), and the estimated viscosity, η , calculated from Eq. (6), using $\eta^0 = 5.13$ mPa·s (the value of the viscosity obtained with the 0.8 charge model) for both solutions.

System	$\log K_1$	$\log K_2$	α	α'	α''	η (mPa·s)
FeCl ₂	-0.20	-1.0	22	56	22	4.46
MgCl ₂	-1.1	-1.9	64	33	3	4.96

* obtained from NIST, Lange's Handbook⁶⁶ or estimated using reasonable guesses; see also Sec. 11 of the SI.

Typically, the values of K are determined from the concentrations at infinite dilution, where the activity coefficients tend towards one. However, at finite concentrations, individual activity coefficients should be estimated, which is usually done using theoretical models, such as SIT^{19–21} (see also Sec. 4.1) or via simulations,⁶⁷ using certain approximations. Note that what is needed is not necessarily each individual activity coefficient, but the right hand side of Eq. (4) or Eq. (5).

It is true that this term is probably not equal to one. Whatever the true value of this term is, one

could consider this term to be effectively incorporated into the value of K_1 and K_2 , thus defining an effective equilibrium constant K_1^* or K_2^* . These are not true thermodynamic equilibrium constants but they are, instead, effective constants that are used with concentrations, and not with activities (they are usually denoted in the literature as stoichiometric equilibrium constants⁶⁸, and in contrast to the true equilibrium constants that depend only on temperature, these constants also depend on the media in which the reaction takes place). In this illustrative calculation, we assume that all values of γ are unity and that Table 7 reports the true equilibrium constant, or that, equivalently, Table 7 reports the values of stoichiometric equilibrium constants K_1^* and K_2^* (with which one would use the concentrations and not activities). In any case, our approach to the problem is meant to be qualitative, rather than quantitative. Moreover, this assumption yielded free cation populations which are in good agreement with the SIT model, when only monomers were considered, as shown in Table 6.

Thus, with the values of the equilibrium constants of Table 7 and using Eq. (6) to predict the viscosity and the results of the force field with the scaled charge 0.8, we obtain a viscosity of 4.46 mPa·s for FeCl₂ (compared to 4.17 mPa·s from our experiments; see Table 2) and 4.96 mPa·s for MgCl₂ (compared to the experimental value of 4.73 mPa·s; see also Sec. 2 in the SI), respectively. Therefore, agreement with experiments is very good, within 5%, which is also consistent with our simulation results. The populations of free ions, monomers and dimers is presented in Table 7. This simple toy model is consistent with the existence of monomers and dimers in FeCl₂ solutions, as shown in recent experiments.^{17,18}

However, we emphasize that we are not claiming that the complex distributions obtained from this calculation correspond to that found in real solutions of FeCl₂ and MgCl₂. We are merely showing how a certain population of complexes would be compatible with the experimental values of the viscosities. Note that there could be several complex distributions that are consistent with the experimental values. The solid orange line in Fig. 5 (which assumes the absence of dimers) is also able to describe the viscosities of both solutions. How-

ever, in every case examined in this work, there is more association in FeCl₂ than in MgCl₂, regardless of the exact proportions of complexes estimated in each solution. In the future, properties such as osmotic coefficients,⁴⁶ freezing point depression,⁶⁹ or electrical conductivities⁷⁰ could be useful for evaluating different speciation possibilities, since we expect them to also be sensitive to the presence of complexes.

4.3 Limitations of empirical force-fields

Most of the ions described up to this point by the Madrid-2019 force-field have an electronic configuration close to that of noble gases (halogen, alkali, alkaline-earth), and for those the model has been relatively successful. Modeling Fe²⁺ with this force-field is the first foray into transition metals which has revealed various challenges and nuances tied to complex formation. An interesting future challenge will be a study of solvated transition metal ions with larger charge, such as Fe³⁺. Recent simulations have shown abrupt switching between two different solvation shell structures, with lifetimes of the order of nanoseconds.⁷¹

However, even with an empirical force-field, it is possible to increase the population of FeCl⁺ monomers with respect to MgCl⁺. This could be accomplished by having different LJ parameters for the Fe–Cl and Mg–Cl interactions. For instance, decreasing the value of σ (the size parameter in the LJ potential), in the first case, with respect to the second, would increase the strength of the Mg–Cl interaction and would consequently increase the population of monomers. This approach was used by Duboué-Dijon et al.²⁶ to increase the number of CIPs in ZnCl₂. Although this methodology is interesting, we believe that it is more fruitful to recognize the limits of empirical force fields to quantitatively describe the energy between a transition metal with several 3 *d* valence electrons and a ligand, and to acknowledge that only an electronic structure calculation can describe this interaction in a quantitative way. Since the required size of a simulated system is large and the computational effort of electronic structure calculations scales rapidly with the number of electrons, a practical approach could involve a hy-

brid simulation method, such as QM/MM (quantum mechanics/molecular mechanics).⁷²

5 Conclusions

The literature contains numerous conflicting reports on complex speciation and the extent of complexation in concentrated FeCl_2 and MgCl_2 solutions. In general, using experiments, theory or simulations to estimate equilibrium complex populations in concentrated solutions is a non-trivial task. However, knowledge of speciation is crucial to understand the behaviour of solutions.

Modelling a transition metal, such as Fe^{2+} , with an empirical force-field is complicated by electronic structure effects (for instance, $3d^6$ configuration). In light of this, the extension of the Madrid-2019 force-field to Fe^{2+} may be deceptively simple, but is a research outcome in its own right.

We have introduced a methodology to incorporate complexes in our simulations which is similar, in spirit, to the seeding method for nucleation,^{73–75} wherein prefabricated critical clusters are introduced. Both methods are characterized by two different timescales: a significantly large one (corresponding to the attainment of the equilibrium complex population in concentrated solutions, in this case, or to the emergence of a critical nucleus in nucleation), and another relatively short timescale of interest (corresponding to transport property calculations as in this work, or to the evolution of a critical cluster in nucleation). Inserting complex populations in simulations of concentrated solutions *a priori* enables us to bypass the computationally prohibitive time required to reach these equilibrium populations. Note that one could obtain information about plausible complex populations from various sources, such as experiments, first principles, and thermodynamics, and subsequently perform simulations using any standard force-field.

We have presented an argument for a strong link between complex distributions and the viscosity, using computer simulations (wherein input complex populations were varied) and with new experimental data for FeCl_2 at high concentration. Although the methods described in this work cannot

quantitatively estimate complex populations, our results provide qualitative information about speciation and show that FeCl_2 has a higher propensity of complexation than MgCl_2 . This could be particularly valuable to obtain clarity about complex speciation when experimental data is elusive or inconclusive.

This idea is not as novel as it may first seem. Weingartner et al.⁹ previously reported experimental viscosity measurements for MgCl_2 and ZnCl_2 , observing that the two systems exhibit very similar viscosities at low concentrations but diverge significantly at higher concentrations. The authors speculated that the formation of complexes caused the lower viscosity of ZnCl_2 . While one cannot change the number of complexes at will in experiments, this can be easily achieved in simulations. In this work, we have demonstrated how complexes can affect the viscosity of solutions at high concentrations, thus confirming the intuition of Weingartner et al.⁹ Nevertheless, further experimental work is required to quantitatively clarify the amount of complexes in concentrated solutions, and NDIS (Neutron Diffraction with Isotopic Substitution^{76–78}), using chloride isotopes in “null” water (a mixture of H_2O and D_2O),⁴⁶ could be particularly informative, especially since the chloride-oxygen chloride-cation peaks would not overlap (expected to be around 3.14 Å and 2.33 Å, respectively). We hope that future research will be continued in this direction, which was first envisaged by Weingartner et al.⁹ more than 40 years ago in this journal.

Supporting Information Available

The authors confirm that the data supporting the findings of this study are available within the article and/or its supplementary materials. A workflow for creating configurations, running LAMMPS simulations and calculating the viscosity can be found at https://github.com/amritagos/electrolyte_workflow. The supporting information contains a description of the simulation methodology for molecular dynamics (MD) simulations, details about the experimental viscosity of MgCl_2 used in this work, an expanded

discussion of the justifications for using the force-field parameters of Mg^{2+} for Fe^{2+} , rationale for the cation-chloride distances chosen to create complexes in simulations (by freezing the distance) and further justifications for this approach, an analysis of solvation shell structures showing that freezing cation-chloride distances does not change the solvation shell, theoretically expected viscosity trends of MgCl_2 and FeCl_2 and details about approximating electrolyte solutions as LJ fluids in order to estimate expected viscosity, predictions of complex speciation from Visual MINTEQ, densities calculated from simulations with and without complexes, a discussion of the slight overestimation of the viscosity by the Madrid-2019 force-field, the effects of complex populations on transport properties, additional details about a back-of-the-envelope calculation for estimating viscosity from Eq. (6), and details of how Jones-Doles B coefficients were estimated using the force-field.

Acknowledgement This work was funded by the Icelandic Research Fund (grants 228615-051 and 2410644-051), and by the Spanish Ministry of Science and Innovation (grants PID2022-136919NB-C31, PID2023-151751NB-I00 and PID2023-147148NB-I00). The calculations were performed using compute resources provided by the Icelandic Research Electronic Infrastructure (IREI). L.F.S. acknowledges an FPU predoctoral Grant No. FPU22/02900. A.G. is grateful to Moritz Sallermann, Rohit Goswami, Alejandro Peña-Torres and Elvar Örn Jónsson for fruitful discussions.

References

- (1) Borodin, O.; Self, J.; Persson, K. A.; Wang, C.; Xu, K. Uncharted waters: Superconcentrated electrolytes. *Joule* **2020**, *4*, 69–100.
- (2) Khalid, S.; Pianta, N.; Mustarelli, P.; Ruffo, R. Use of water-in-salt concentrated liquid electrolytes in electrochemical energy storage: State of the art and perspectives. *Batteries* **2023**, *9*, 47.
- (3) Han, J.; Mariani, A.; Passerini, S.; Varzi, A. A perspective on the role of anions in highly concentrated aqueous electrolytes. *Energy Environ. Sci.* **2023**, *16*, 1480–1501.
- (4) Luin, U.; Valant, M. Electrolysis energy efficiency of highly concentrated FeCl_2 solutions for power-to-solid energy storage technology. *J. Solid State Electrochem.* **2022**, *26*, 929–938.
- (5) Millero, F. J. Seawater as a multicomponent electrolyte solution. *Mar. Chem.* **1974**, *5*, 3–80.
- (6) Osterhout, W. How do electrolytes enter the cell? *Proc. Natl. Acad. Sci. U.S.A.* **1935**, *21*, 125–132.
- (7) Debye, P.; Huckel, E. On the theory of electrolytes. I. Freezing point depression and related phenomena. *Phys. Z.* **1923**, *24*, 185–206.
- (8) Panagiotopoulos, A. Z. Simulations of activities, solubilities, transport properties, and nucleation rates for aqueous electrolyte solutions. *J. Chem. Phys.* **2020**, *153*, 010903.
- (9) Weingartner, H.; Muller, K. J.; Hertz, H. G.; Edge, A. V. J.; Mills, R. Unusual behavior of transport coefficients in aqueous solutions of Zinc Chloride at 25 °C. *J. Phy. Chem.* **1984**, *88*, 10.
- (10) Wells, C.; Salam, M. A. Complex formation between Fe(II) and inorganic anions. Part 1.—Effect of simple and complex halide ions on the $\text{Fe(II)}+\text{H}_2\text{O}_2$ reaction. *Trans. Faraday Soc.* **1967**, *63*, 620.
- (11) Böhm, F.; Sharma, V.; Schwaab, G.; Havenith, M. The low frequency modes of solvated ions and ion pairs in aqueous electrolyte solutions: iron(II) and iron(III) chloride. *Phys. Chem. Chem. Phys.* **2015**, *17*, 19582–19591.
- (12) Martell, A. E.; Smith, R. M. *Critical stability constants*; Springer, 1974; Vol. 1.
- (13) Arnorsson, S.; Sigurdsson, S.; Svavarsson, H. The chemistry of geothermal waters

- in Iceland. I. Calculation of aqueous speciation from 0 to 370 °C. *Geochim. Cosmochim. Acta* **1982**, *46*, 1513.
- (14) Ruaya, J. R. Estimation of instability constants of metal chloride complexes in hydrothermal solutions up to 300 °C. *Geochim. Cosmochim. Acta* **1988**, *52*, 1983.
- (15) Heinrich, A.; Seward, T. M. A spectrophotometric study of aqueous iron (II) chloride complexing from 25 to 200 °C. *Geochim. Cosmochim. Acta* **1990**, *54*, 2207.
- (16) Palmer, D. A.; Hyde, K. E. An experimental determination of ferrous chloride and acetate complexation in aqueous solutions to 300 °C. *Geochim. Cosmochim. Acta* **1993**, *57*, 1393.
- (17) Zhao, R.; Pan, P. A spectrophotometric study of Fe(II)-chloride complexes in aqueous solutions from 10 to 100 °C. *Can. J. Chem.* **2001**, *79*, 131–144.
- (18) Luin, U.; Arčon, I.; Valant, M. Structure and population of complex ionic species in FeCl₂ aqueous solution by X-ray absorption spectroscopy. *Molecules* **2022**, *27*, 642.
- (19) Bronsted, J. N. Studies on solubility IV. The principle of the specific interaction of ions. *J. Am. Chem. Soc.* **1922**, *44*, 877.
- (20) Guggenheim, E.; Turgeon, J. Specific interaction of ions. *Trans. Faraday Soc.* **1955**, *51*, 747.
- (21) Ciavatta, L. The specific interaction theory in the evaluating ionic equilibria. *Trans. Faraday Soc.* **1980**, *70*, 551.
- (22) Davies, C. W. 397. The extent of dissociation of salts in water. Part VIII. An equation for the mean ionic activity coefficient of an electrolyte in water, and a revision of the dissociation constants of some sulphates. *J. Chem. Soc.* **1938**, *8*, 2093.
- (23) Gustafsson, J. P. Visual MINTEQ 3.0 user guide. *KTH, Department of Land and Water Resources, Stockholm, Sweden* **2011**, 550.
- (24) Marcus, Y. The anion exchange of metal complexes—IV. *J. Inorg. Nucl. Chem.* **1960**, *12*, 287–296.
- (25) Tagirov, B. R.; Diakonov, I. I.; Devina, O. A.; Zotov, A. V. Standard ferric–ferrous potential and stability of FeCl₂²⁺ to 90°C. Thermodynamic properties of Fe_(aq)³⁺ and ferric-chloride species. *Chem. Geol.* **2000**, *162*, 193–219.
- (26) Duboué-Dijon, E.; Mason, P. E.; Fischer, H. E.; Jungwirth, P. Hydration and ion pairing in aqueous Mg²⁺ and Zn²⁺ solutions: Force-field description aided by neutron scattering experiments and ab initio molecular dynamics simulations. *J. Phys. Chem. B* **2017**, *122*, 3296–3306.
- (27) Zapałowski, M.; Bartczak, W. M. Concentrated aqueous MgCl₂ solutions. A computer simulation study of the solution structure and excess electron localisation. *Res. Chem. Intermed.* **2001**, *27*, 855–866.
- (28) Dai, Q.; Xu, J.-J.; Li, H.-J.; Yi, H.-B. Ion association characteristics in MgCl₂ and CaCl₂ aqueous solutions: a density functional theory and molecular dynamics investigation. *Mol. Phys.* **2015**, *113*, 3545–3558.
- (29) Feng, G.; Liu, C.-W.; Zeng, Z.; Hou, G.-L.; Xu, H.-G.; Zheng, W.-J. Initial hydration processes of magnesium chloride: size-selected anion photoelectron spectroscopy and ab initio calculations. *Phys. Chem. Chem. Phys.* **2017**, *19*, 15562–15569.
- (30) Zeron, I.; Abascal, J.; Vega, C. A force field of Li⁺, Na⁺, K⁺, Mg²⁺, Ca²⁺, Cl⁻, and SO₄²⁻ in aqueous solution based on the TIP4P/2005 water model and scaled charges for the ions. *J. Chem. Phys.* **2019**, *151*, 134504.
- (31) National Institute of Standards and Technology (NIST) NIST SRD 46: Critically Selected Stability Constants of Metal Complexes (NIST46), Version 8.0. NIST Standard Reference Data, Accessed: 2026-02-26.

- (32) Callahan, K. M.; Casillas-Ituarte, N. N.; Roeselová, M.; Allen, H. C.; Tobias, D. J. Solvation of Magnesium Dication: Molecular Dynamics Simulation and Vibrational Spectroscopic Study of Magnesium Chloride in Aqueous Solutions. *J. Phys. Chem. A* **2010**, *114*, 5141–5148.
- (33) Sanmamed, Y. A.; Dopazo-Paz, A.; González-Salgado, D.; Troncoso, J.; Romani, L. An accurate calibration method for high pressure vibrating tube densimeters in the density interval (700 to 1600) kg·m⁻³. *J. Chem. Thermodyn.* **2009**, *41*, 1060–1068.
- (34) Blazquez, S.; Troncoso, J.; La Francesca, P.; Gallo, P.; Conde, M.; Vega, C. Extending the Madrid-2019 force field to the perchlorate anion: role of charge distribution and validation with experiments on Mars-relevant aqueous solutions. *J. Mol. Liq.* **2025**, *435*, 128035.
- (35) Laliberté, M.; Cooper, W. E. Model for calculating the density of aqueous electrolyte solutions. *J. Chem. Eng. Data* **2004**, *49*, 1141–1151.
- (36) Laliberté, M. Model for calculating the viscosity of aqueous solutions. *J. Chem. Eng. Data* **2007**, *52*, 321–335.
- (37) Abraham, M. J.; Murtola, T.; Schulz, R.; Páll, S.; Smith, J. C.; Hess, B.; Lindahl, E. GROMACS: High performance molecular simulations through multi-level parallelism from laptops to supercomputers. *SoftwareX* **2015**, *1–2*, 19–25.
- (38) Thompson, A. P.; Aktulga, H. M.; Berger, R.; Bolintineanu, D. S.; Brown, W. M.; Crozier, P. S.; Veld, P. J. I. '.; Kohlmeyer, A.; Moore, S. G.; Nguyen, T. D.; Shan, R.; Stevens, M. J.; Tranchida, J.; Trott, C.; Plimpton, S. J. LAMMPS - a flexible simulation tool for particle-based materials modeling at the atomic, meso, and continuum scales. *Comput. Phys. Commun.* **2022**, *271*, 108171.
- (39) Abascal, J. L. F.; Vega, C. A general purpose model for the condensed phases of water: TIP4P/2005. *J. Chem. Phys.* **2005**, *123*, 234505.
- (40) Leontyev, I. V.; Stuchebrukhov, A. A. Electronic continuum model for molecular dynamics simulations. *J. Chem. Phys.* **2009**, *130*, 085102.
- (41) Leontyev, I. V.; Stuchebrukhov, A. A. Electronic continuum model for molecular dynamics simulations of biological molecules. *J. Chem. Theory Comput.* **2010**, *6*, 1498–1508.
- (42) Kirby, B. J.; Jungwirth, P. Charge scaling manifesto: A way of reconciling the inherently macroscopic and microscopic natures of molecular simulations. *J. Phys. Chem. Lett.* **2019**, *10*, 7531–7536.
- (43) Cruces Chamorro, V.; Jungwirth, P.; Martinez-Seara, H. Building water models compatible with charge scaling molecular dynamics. *J. Phys. Chem. Lett.* **2024**, *15*, 2922–2928.
- (44) Jorge, M.; Lue, L. The dielectric constant: Reconciling simulation and experiment. *J. Chem. Phys.* **2019**, *150*, 084108.
- (45) Le Breton, G.; Joly, L. Molecular modeling of aqueous electrolytes at interfaces: Effects of long-range dispersion forces and of ionic charge rescaling. *J. Chem. Phys.* **2020**, *152*, 241102.
- (46) Biriukov, D.; Wang, H.-W.; Rampal, N.; Tempra, C.; Kula, P.; Neufeind, J. C.; Stack, A. G.; Predota, M. The good, the bad, and the hidden in neutron scattering and molecular dynamics of ionic aqueous solutions. *J. Chem. Phys.* **2022**, *156*, 194505.
- (47) Blazquez, S.; Conde, M.; Vega, C. Scaled charges for ions: An improvement but not the final word for modeling electrolytes in water. *J. Chem. Phys.* **2023**, *158*, 054505.
- (48) Chou, I. M.; Phan, L. D. Solubility relations in the system sodium chloride-ferrous

- chloride-water between 25 and 70.degree.C at 1 atm. *J. Chem. Eng. Data* **1985**, *30*, 216–218.
- (49) Marcus, Y. *Ion Properties*; Marcel Dekker, Inc., 1997.
- (50) Jenkins, H. D. B.; Marcus, Y. Viscosity B-Coefficients of Ions in Solution. *Chem. Rev.* **1995**, *95*, 2695.
- (51) Wang, P.; Anderko, A.; Young, R. D. Modeling viscosity of concentrated and mixed-solvent electrolyte systems. *Fluid Ph. Equilib.* **2004**, *226*, 71–82.
- (52) Patil, R. S.; Shaikh, V. R.; Patil, P. D.; Borse, A. U.; Patil, K. J. The viscosity B and D coefficient (Jones–Dole equation) studies in aqueous solutions of alkyltrimethylammonium bromides at 298.15 K. *J. Mol. Liq.* **2014**, *200*, 416–424.
- (53) Bruni, F.; Imberti, S.; Mancinelli, R.; Ricci, M. A. Aqueous solutions of divalent chlorides: ions hydration shell and water structure. *J. Chem. Phys.* **2012**, *136*, 064520.
- (54) Friesen, S.; Hefter, G.; Buchner, R. Cation Hydration and Ion Pairing in Aqueous Solutions of MgCl₂ and CaCl₂. *J. Phys. Chem. B* **2019**, *123*, 891–900.
- (55) Zhang, W.; Van Duin, A. C. Second-generation ReaxFF water force field: improvements in the description of water density and OH-anion diffusion. *J. Phys. Chem. B* **2017**, *121*, 6021–6032.
- (56) Burgess, J. *Metal ions in solution*; Ellis Horwood limited, 1978.
- (57) Burgess, J. *Ions in solutions : basic principles of chemical interactions*; Ellis Horwood limited, 1988.
- (58) Yue, S.; Panagiotopoulos, A. Z. Dynamic properties of aqueous electrolyte solutions from non-polarisable, polarisable, and scaled-charge models. *Mol. Phys.* **2019**, *117*, 3538–3549.
- (59) Elliott, G. R.; Wanless, E. J.; Webber, G. B.; Andersson, G. G.; Craig, V. S. J.; Page, A. J. Dynamic Ion Correlations and Ion-Pair Lifetimes in Aqueous Alkali Metal Chloride Electrolytes. *J. Phys. Chem. B* **2024**, *128*, 7438–7444.
- (60) Pye, C. C.; Rudolph, W. An ab initio and Raman investigation of magnesium (II) hydration. *J. Phys. Chem. A* **1998**, *102*, 9933–9943.
- (61) Yeh, I.; Hummer, G. System-size dependence of diffusion coefficients and viscosities from molecular dynamics simulations with periodic boundary conditions. *J. Phys. Chem. B* **2004**, *108*, 15873–15879.
- (62) Shi, R.; Cooper, A. J.; Tanaka, H. Impact of hierarchical water dipole orderings on the dynamics of aqueous salt solutions. *Nat. Commun* **2023**, *14*, 4616.
- (63) McCall, D. W.; Douglass, D. C. The Effect of Ions on the Self-Diffusion of Water. I. Concentration Dependence. *J. Phys. Chem.* **1965**, *69*, 2001.
- (64) Blazquez, S.; Zeron, I.; Conde, M.; Abascal, J.; Vega, C. Scaled charges at work: Salting out and interfacial tension of methane with electrolyte solutions from Computer simulations. *Fluid Ph. Equilib* **2020**, *513*, 112548.
- (65) Fan, S.; Mason, P. E.; Chamorro, V. C.; Shanks, B. L.; Martinez-Seara, H.; Jungwirth, P. Charge scaling force field for biologically relevant ions utilizing a global optimization method. *J. Chem. Theory Comput.* **2025**, *21*, 9023.
- (66) Dean, J. A. *Lange’s Handbook of Chemistry, 15th Edition*; McGraw-Hill: New York, 1999.
- (67) Saravi, S. H.; Panagiotopoulos, A. Z. Individual ion activity coefficients in aqueous electrolytes from explicit-water molecular dynamics simulations. *J. Phys. Chem. B* **2021**, *125*, 8511.

- (68) Zeebe, R. E.; Wolf-Gladrow, D. *CO₂ in seawater: equilibrium, kinetics, isotopes*; Elsevier Oceanography Series, 2001.
- (69) Lamas, C. P.; Vega, C.; Noya, E. G. Freezing point depression of salt aqueous solutions using the Madrid-2019 model. *J. Chem. Phys.* **2022**, *156*, 134503.
- (70) Blazquez, S.; Abascal, J. L.; Lagerweij, J.; Habibi, P.; Dey, P.; Vlugt, T. J.; Moulτος, O. A.; Vega, C. Computation of electrical conductivities of aqueous electrolyte solutions: Two surfaces, one property. *J. Chem. Theory Comput.* **2023**, *19*, 5380–5393.
- (71) Goswami, A.; Peña-Torres, A.; Jónsson, E. O.; Egorov, S. A.; Jónsson, H. Evidence of sharp transitions between octahedral and capped trigonal prism states of the solvation shell of the aqueous Fe³⁺ ion. *J. Phys. Chem. Lett.* **2024**, *15*, 4523–4530.
- (72) Kirchhoff, B.; Jónsson, E. O.; Dohn, A. O.; Jacob, T.; Jónsson, H. Elastic collision based dynamic partitioning scheme for hybrid simulations. *J. Chem. Theory Comput.* **2021**, *17*, 5863–5875.
- (73) Espinosa, J. R.; Vega, C.; Valeriani, C.; Sanz, E. Seeding approach to crystal nucleation. *J. Chem. Phys.* **2016**, *144*, 034501.
- (74) Bai, X.-M.; Li, M. Calculation of solid-liquid interfacial free energy: A classical nucleation theory based approach. *J. Chem. Phys.* **2006**, *124*, 124707.
- (75) Goswami, A.; Dalal, I. S.; Singh, J. K. Seeding method for ice nucleation under shear. *J. Chem. Phys.* **2020**, *153*, 094502.
- (76) Neilson, G. W.; Tromp, R. H. Neutron and X-ray diffraction on aqueous solutions. *Annu. Rep. Prog. Chem., Sect. C: Phys. Chem.* **1991**, *88*, 45.
- (77) Enderby, J. E. Ion solvation via neutron scattering. *Chem. Soc. Rev.* **1995**, *24*, 159.
- (78) Neilson, G. W.; Enderby, J. E. Aqueous solutions and neutron scattering. *J. Phys. Chem.* **1996**, *100*, 1317.

Supporting Information

Viscosity as a Smoking Gun for Complex Formation in Solution: Fe²⁺ and Mg²⁺ Chlorides as Examples

Amrita Goswami, Samuel Blazquez, Lucía Fernández-Sedano Vázquez, Eva González Noya, Hannes Jónsson, Jacobo Troncoso, Carlos Vega

S1 Simulation methods	19
S1.1 Simulation details	19
S1.1.1 GROMACS	20
S1.1.2 LAMMPS	20
S1.2 Configuration generation with complexes and energy minimization	20
S1.3 Viscosity calculations from simulations	20
S2 Experimental viscosities of MgCl₂	21
S3 Justification for the Fe²⁺ force-field parameters	22
S4 Justification for chosen cation-chloride distances and for rigid bonds	23
S5 Validation of simulation protocol with rigid cation-chloride bonds	24
S6 Theoretically expected viscosity trends of FeCl₂ and MgCl₂	24
S7 Predictions of speciation from chemical equilibrium models	25
S8 Densities from simulations	26
S8.1 Simulations without complexes	26
S8.2 Simulations incorporating complexes	26
S9 Overestimation of viscosities by Madrid-2019	27
S10 Speciation effects on transport properties	27
S11 Back-of-the-envelope calculation for viscosities	29
S12 Evaluation of the Jones-Dole coefficient of a force-field	30
References	31

S1 Simulation methods

In this work, we have extended the Madrid-2019 force-field^{S1} to the Ferrous ion, Fe^{2+} , using the same parameters as for Mg^{2+} . The Madrid-2019 force-field combines the TIP4P/2005 model of water^{S2} with scaled charges for the ions. The proposed force-field parameters are collected in Table 1 in the main text. Parameters for Mg^{2+} , Cl^- can be found in our previous work^{S1} and those of perchlorate from our recent work.^{S3} Note that the canonical Madrid-2019 force-field^{S1} uses a scaled charge of $0.85 e$. It is well-known that the Madrid-2019 force-field tends to overestimate the viscosities of electrolytes in water (even for NaCl, KCl where contact ion pairs, but no complexes, are formed), as described further in Sec S9. It has been proposed that lowering the charge to 0.8 reduces many of the discrepancies with experiments (and with 0.75 it is even possible to reproduce the experimental results).^{S4} For this reason, we have also performed analyses using a scaled charge of 0.8. The change of the charge of the ions requires some adjustment of the Lennard-Jones (LJ) parameters (simply replacing the charge and keeping the LJ parameters optimized for the $q = 0.85 e$ model is not a good option^{S4}). For the model with $q = 0.8 e$, the value of σ for the $\text{Cl}-\text{O}_w$ was taken from our previous work Ref.^{S4} and the value of LJ σ for the $\text{Fe}^{2+}-\text{O}_w$ or $\text{Mg}^{2+}-\text{O}_w$ was optimized in this work, obtaining $\sigma = 1.85 \text{ \AA}$, as shown in Table 1 in the main text.

Regarding FeCl_2 simulations, it is important to consider the possibility of Fe^{2+} undergoing a certain amount of hydrolysis in water. However, in this work, for the highest concentration (4 m), the pH is about 5. Therefore, the concentration of H_3O^+ and $\text{Fe}(\text{OH})^+$ is quite small (of the order of about 10^{-5} m) and can be neglected when performing simulations to describe this system.

We have used the molality scale, m , for concentrations (mol of salt per kg of water) as is typically done in experimental studies, since the concentration then does not depend on the volume of the system. Furthermore, in simulations we typically used 555 molecules of water to determine the densities of the aqueous ionic solutions (and multiples of the same for viscosity simulations). This is very convenient, since then 1 m or 2 m solutions are obtained with 10 or 20 molecules of salt.

S1.1 Simulation details

Simulations were performed using the GROMACS (version 2025.2)^{S5} and LAMMPS (29 Aug 2024, Update 1)^{S6} packages. Specific simulation details for GROMACS and LAMMPS are provided in Sec. S1.1.1 and Sec. S1.1.2, respectively.

Densities were computed from NpT simulations, with 555 water molecules, run for 50 ns each. Prior to production runs, the simulations were equilibrated for 10 ns.

For the viscosity calculations, each independent configuration contained 4440 water molecules, within a box size corresponding to the averaged density for each concentration. Note that independent configurations were created using the methodology described in Sec. S1.2. Viscosities were computed from 8 – 15 independent simulation runs in the NVT ensemble, using both LAMMPS and GROMACS, which were subsequently averaged (over a total of 16 – 30 independent simulations). Each independent simulation was run for 40-50 ns (following a 4 ns simulation of simulated annealing and subsequently a 20 ns period of equilibration).

The diffusion coefficient was calculated from unwrapped coordinate trajectories generated during the viscosity calculations in the NVT ensemble. The Yeh-Hummer correction^{S7} was applied to the diffusion coefficients to account for finite-size effects.

A workflow for creating configurations, running LAMMPS simulations and calculating the viscosity can be found at https://github.com/amritagos/electrolyte_workflow. Snapshots and visuals were created using solvis (<https://github.com/amritagos/solvis>).

S1.1.1 GROMACS

In GROMACS, simulations were performed in the NpT ensemble with a Nose-Hoover thermostat^{S8} and the barostat from Parrinello-Rahman.^{S9,S10} The time step was of 2 fs. Ewald sums (PME) were used for the long-range electrostatic interactions in GROMACS. A long-range correction to the LJ part of the potential was added. The potential was truncated at 10 Å. The shape of the water molecules was constrained using the LINCS algorithm^{S11}. In the case of complexes, the cation-anion distance was also frozen using LINCS (see also Sec.S4 and Sec.S5).

S1.1.2 LAMMPS

Analogous simulations in LAMMPS were performed using the Nose-Hoover thermostat^{S8} and Nose-Hoover barostat,^{S12} with a thermostat and barostat coupling constant of 200 fs and 5 ps, respectively. Likewise, the timestep used was 2 fs. Long-range electrostatics were computed using particle-particle particle-mesh (PPPM).^{S13} Similar to the protocol in GROMACS, long-range corrections to the LJ terms were added, and a cutoff of 10 Å was used. The SHAKE algorithm^{S14} was used to constrain the shape of water molecules and to constrain the cation-anion distances in complexes (see also Sec.S4 and Sec.S5).

S1.2 Configuration generation with complexes and energy minimization

As part of our new simulation strategy of studying transport properties at a static predetermined complex population (see Sec.S4 and Sec.S5 for justification and validation), we perform simulations in which we artificially maintain the desired complex population. This is accomplished by constraining the cation-anion distance in simulations of FeCl₂ and MgCl₂. Concerning configuration generation, usually it is trivial to create initial configurations using tools such as PACKMOL^{S15} or Moltemplate.^{S16} However, especially for concentrated systems, and in the situations where we insert complexes, configuration creation can be a slightly more involved process. In this work, a *monomer* refers to a complex formed by one cation, coordinated with one Cl⁻ anion and some additional molecules of water in the first solvation shell, while a *dimer* refers to a complex wherein there are two Cl⁻ anions in the trans position of the octahedron, and some additional coordinating water molecules (see Fig.2 in the main text). In the case of a "monomer" or "dimer" complex, a unit consisting of a bonded metal ion and chloride, or a "triatomic" unit consisting of two chlorides and one metal ion was created. Each species was randomly distributed in the simulation box, keeping a tolerance of 3.0 Å between complexes. A Python program was written for this purpose which uses PACKMOL, Moltemplate and Atomic Simulation Environment (ASE)^{S17}, under the hood; see <https://github.com/amritagos/confi>. Certain typical file formats in LAMMPS and GROMACS can also be converted using `confi`.

Configurations were created in the manner described above in order to facilitate subsequent energy minimization. Energy minimization with the aforementioned complexes was performed by keeping the complexes frozen and only allowing the water molecules to move. However, in the case of free cations and anions, all atoms were allowed to move. The energy was minimized in two stages– first with 1000 steps of steepest descent, followed by a maximum of 10000 steps of the conjugate gradient algorithm, with a step size of 0.001 fs.

S1.3 Viscosity calculations from simulations

Using the Green-Kubo formalism, the viscosity is obtained from the expression:

$$\eta = \frac{V}{k_B T} \int_0^\infty \langle P_{\lambda\beta}(\tau) P_{\lambda\beta}(0) \rangle d\tau, \quad (\text{S1})$$

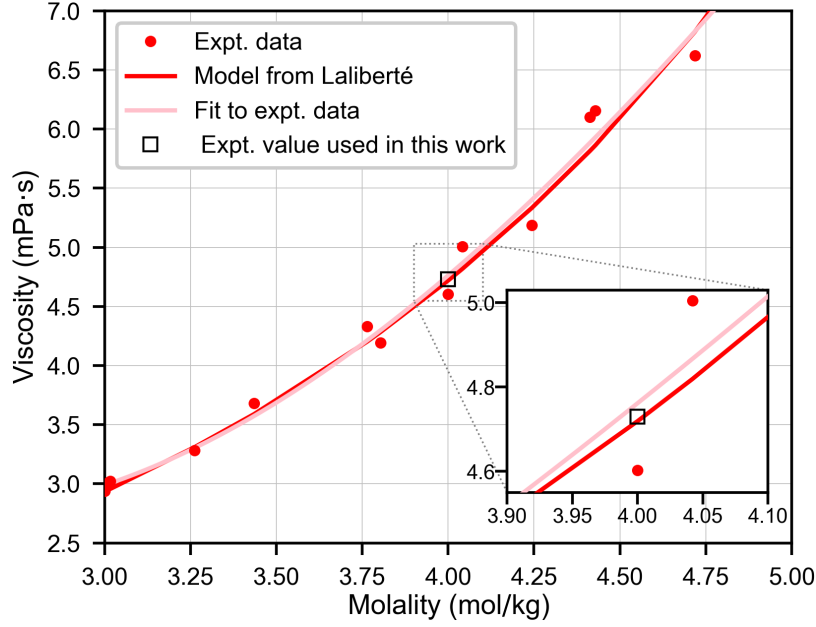


Figure S1: Viscosities of MgCl_2 from experiments^{S19} (filled red circles), model fitted to experimental data points^{S19} (solid red line), along with a fit to experimental data points in the interval 3 m to 5 m (solid pink line). The experimental value of the viscosity used in this work at 4 m is denoted by an open square. The inset shows a zoomed-in view close to 4 m.

with k_B the Boltzmann constant, V is the volume, T is the temperature and $P_{\lambda\beta}$ are the non diagonal components of the pressure tensor (i.e., $\lambda \neq \beta$) which are given as:

$$\begin{aligned}
P_{\lambda\beta}(\tau) &= \frac{1}{V} \sum_{i=1}^N m_i v_{\lambda,i}(\tau) v_{\beta,i}(\tau) \\
&+ \frac{1}{V} \sum_{i=1}^N r_{\lambda,i}(\tau) f_{\beta,i}(\tau) \\
&= P_{\lambda\beta}^K + P_{\lambda\beta}^U,
\end{aligned} \tag{S2}$$

where $v_{\lambda,i}$, $r_{\lambda,i}$ and $f_{\lambda,i}$ denote the λ component of the velocity, position and force acting on particle i respectively. The first term of Eq. (S2) is a kinetic term that depends on the masses of the particles of the system, and the second term is a virial term that only depends on positions and forces, but not on masses. The sum in Eq. (S2) is over the N particles of the system (water and ions, in our case). The three non diagonal components and the terms $\frac{1}{2}(P_{xx} - P_{yy})$ and $\frac{1}{2}(P_{yy} - P_{zz})$ were used to get the correlation function of the pressure tensor as in the work of Gonzalez and Abascal^{S18}. The pressure tensor can be divided into a kinetic contribution K , and a potential energy contribution U as shown in Eq. (S2). Therefore when using the Green-Kubo formula one has a KK contribution, a KU contribution and a UU contribution.

S2 Experimental viscosities of MgCl_2

As shown in Fig. S1, individual experimental measurements (red circles) are scarce and rather scattered. Therefore, Laliberté^{S19} has proposed a model that fits to the existing experimental data (solid red line in Fig. S1). In this work, we have performed a detailed study at 4 m. Therefore, we have also fitted to the experimental data in the range 3-5 m. Using the model from Laliberté^{S19} and our own fit, we settle on a viscosity of 4.73 mPa·s for MgCl_2 at 4 m. Subsequently, we have used this value in this work as the

experimental value of MgCl_2 .

S3 Justification for the Fe^{2+} force-field parameters

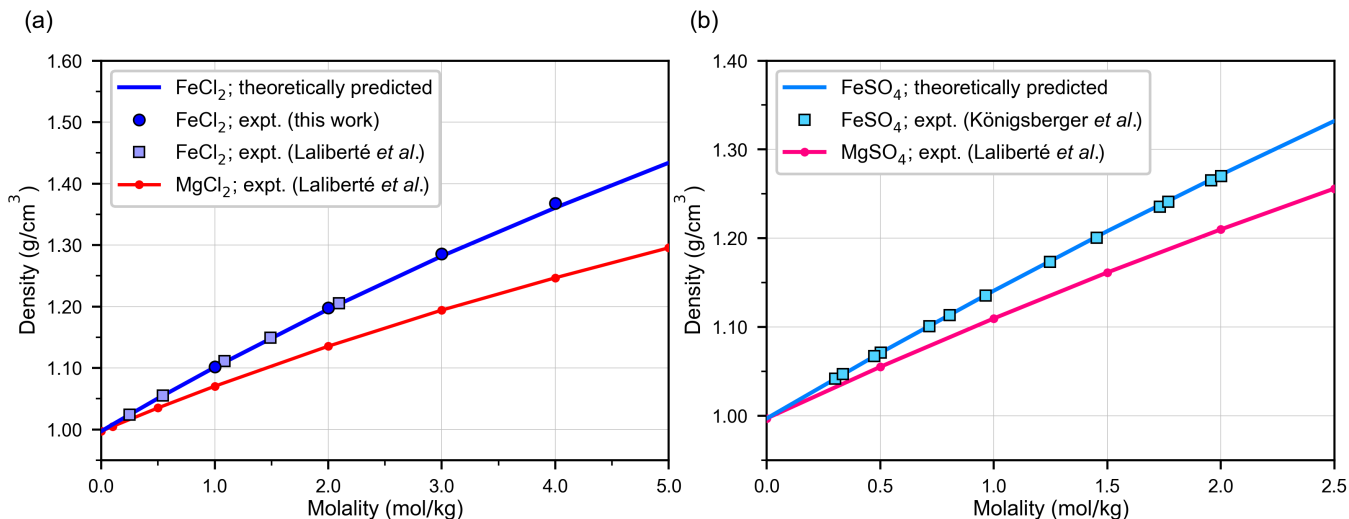


Figure S2: (a) Experimental densities of FeCl_2 (light-blue symbols and blue symbols for results from Laliberté and Cooper^{S20} and results from this work, respectively), as well as experimental densities of MgCl_2 (red line). Assuming equal volumes for the FeCl_2 and MgCl_2 solutions, we obtain the solid blue line as the predicted density of FeCl_2 . (b) Densities of FeSO_4 and MgSO_4 from experiments, and those scaled by assuming equal volumes. Densities of FeSO_4 were taken from Königsberger *et al.*^{S21}, and those of MgSO_4 from Laliberté and Cooper^{S20}.

Fig. S2(a) presents the densities of FeCl_2 and MgCl_2 obtained from experiments, including the experimental results of this work (see also Table 2 of the main text). As can be gleaned from Fig. S2(a), the mass densities of FeCl_2 and MgCl_2 are clearly different.

Using the approximation of equal number densities (Eq. 1 in the main text), we can theoretically estimate the mass density of FeCl_2 , using the experimentally calculated mass densities of MgCl_2 . Fig. S2(a) shows that the theoretically predicted mass densities of FeCl_2 (assuming that MgCl_2 and FeCl_2 have the same number density) agree well with the densities from experiments. We show that a similar approximation can be made for FeSO_4 and MgSO_4 solutions in Fig. S2(b).

This is a promising sign that the same force-field parameters as Mg^{2+} could be used for Fe^{2+} .

Table S1: Metal – O_w distances, $d_{\text{M}-\text{O}_w}$ (in Å), and hydration free energies (in kcal/mol).

	$d_{\text{M}-\text{O}_w}$	HFE
$\text{Mg}^{2+} - \text{O}_w$	2.11 ± 0.01^b	-437.4^c
$\text{Fe}^{2+} - \text{O}_w$	2.095^a 2.09 ± 0.04^b	-439.8^c

* a) From Uroš Luin *et al.*^{S22} b) Collected in Ohtaki and Radnai^{S23}, Marcus^{S24} c) From Marcus^{S25}

We believe that this is further justified by the fact that the experimentally measured cation-oxygen distance^{S26} is similar for Mg^{2+} and Fe^{2+} , as shown in Table S1. Table S1 also presents the hydration free

energies, which are almost identical for both ions. Therefore, we surmise that the cation-water interactions for both cations are similar, both in terms of the distance and magnitude of the interaction energy. Following on this premise, we conclude that a suitable force-field for Mg^{2+} should work reasonably well for Fe^{2+} .

Note that when the same force-field is used to describe Mg^{2+} and Fe^{2+} , despite having different masses, classical simulations should necessarily yield the same thermodynamic properties such as the hydration free energy, radial distribution functions, surface tension, activity coefficients and freezing point depression. This is a consequence of using classical statistical thermodynamics. However, transport properties are affected by the mass and are, therefore, expected to be different.

S4 Justification for chosen cation-chloride distances and for rigid bonds

Table S2: Bond length distances, $d_{\text{M-Cl}}$, (in Å) in the metal ion chloride (M–Cl) complexes.

System	$d_{\text{M-Cl}}$
$\text{Mg}^{2+}\text{-Cl}$	2.30 ^a , 2.55 ^b
$\text{Fe}^{2+}\text{-Cl}$	2.33 ^c
$\text{Fe}^{3+}\text{-Cl}$	2.30 ^d

* a) From a simulation study by Zapałowski and Bartczak^{S27} b) From an experimental study of $\text{MgCl}_2(\text{H}_2\text{O})_4$ by Schmidt et al.^{S28} c) From Uroš Luin et al.^{S22} d) From Lind^{S29}

It has been shown that when the metal–water oxygen distance (M-O_w) is similar for two cations, their corresponding metal–chloride (M-Cl) distances are also comparable. For example, Kuppuraj et al.^{S30} demonstrated this relationship for the divalent cations Co^{2+} and Fe^{2+} .

Metal–chloride distances for a range of divalent metal ions are reported in Refs.^{S31,S32} and are summarized in Table S2. These data show that the M-Cl bond lengths for Fe^{2+} and Mg^{2+} fall within a narrow range.

On this basis, we adopt the same metal–chloride bond distance for both the Fe-Cl and Mg-Cl complexes, setting $\text{M-Cl} = 2.33$ Å. Note that, in our new simulation approach, cation-anion distances are constrained to the same value using either the SHAKE^{S14} or LINCS^{S11} algorithms.

We justify this new approach of freezing ion pairs in the following. The lifetime of the cation-anion pair (complexes) in FeCl_2 and MgCl_2 is of the order of microseconds.^{S33} Note that this means that a chloride ion cannot leave the Fe^{2+} or Mg^{2+} cation within our simulation time scales. However, insofar as the viscosity is concerned, a lifetime greater than ≈ 100 ps could be effectively considered "intransient" or "stable". This is because the Green-Kubo integral reaches a plateau, and that indicates that the integrand, which gives the correlation function of the non-diagonal pressure tensor components, goes to zero, as can be seen from the inset of Fig. 1 in the main text. Thus, if the residence time of a cation and an anion is less than 100 ps (which is the case for aqueous NaCl , KCl or RbCl), then it is a labile contact ion pair, and it is more useful to consider it as a fluctuation within the configurational space.

As touched upon previously, the stability of long-lived complexes formed in FeCl_2 and MgCl_2 implies that reaching the equilibrium chemical composition can take of the order of microseconds to seconds (especially if the empirical force-field, or even an *ab-initio* simulation, mimics the experimental relaxation

times, in a realistic way, which is desirable). When using the Madrid-2019 force-field, the formation of complexes is not observed even after 200 ns runs (i.e., the cation and anion were not in contact, in both the initial and in the final configurations).

S5 Validation of simulation protocol with rigid cation-chloride bonds

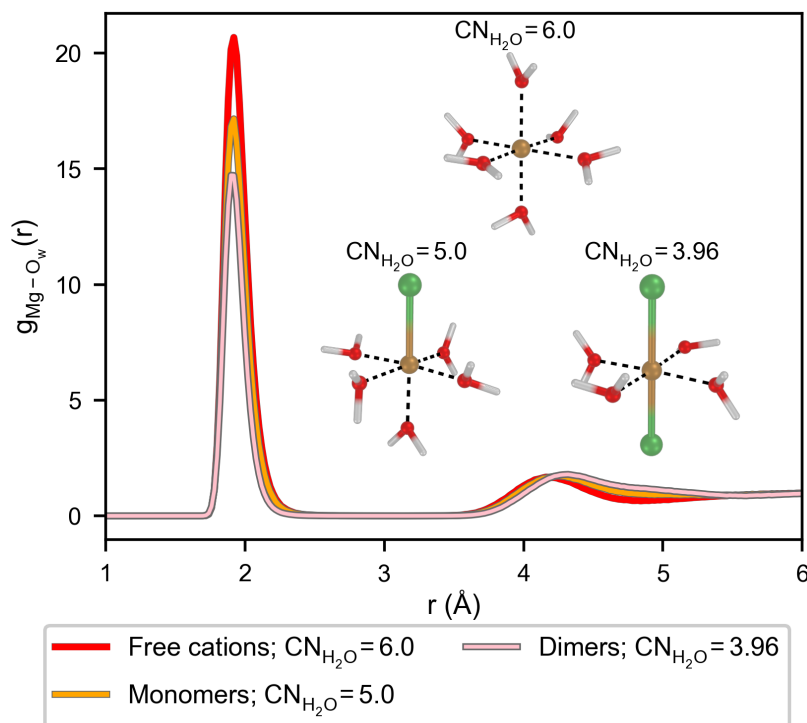


Figure S3: Radial distribution function between Mg^{2+} and the oxygen atoms in water obtained from simulations using free ions (red curve), the monomer complex (yellow curve), the dimer complex (pink curve), and the water coordination number ($\text{CN}_{\text{H}_2\text{O}}$) at 4 m. The total coordination number (including both the water molecules and chloride ions in the first solvation shell) is close to 6.0 in all cases. Insets depict typical solvation shells for free cations, monomers and dimers.

To assess the validity of the aforementioned simulation strategy, we analyzed the structures of the solvation shell around free cations, monomers and dimers. The radial distribution functions between Mg^{2+} and O_w , for free cations, monomers and dimers, at a concentration of 4 m are shown in Fig. S3. The expected solvation structure around both Mg^{2+} and Fe^{2+} is octahedral.^{S23,S34} If this structure is retained by the monomers and dimers, the total coordination number should be close to 6.0. Since we obtain hydration numbers of 5.0 and 3.96 for monomers and dimers, respectively, as shown in Fig. S3, we can conclude that constraining the cation-chloride distance does not distort the solvation shell around the cation.

S6 Theoretically expected viscosity trends of FeCl_2 and MgCl_2

From Fig.2 in the main text, it is evident that while the viscosities of MgCl_2 and FeCl_2 are similar at low concentration, upto 2 m, they diverge greatly at higher concentration. From experiments, the viscosity of FeCl_2 at 4 m is 4.17 mPa.s (Table 1 in the main text), compared to that of MgCl_2 at the same concentration,

equal to 4.73 mPa.s (see also Sec. S2). In the main text, we conclude that the formation of complexes (greater in FeCl₂ compared to MgCl₂) is responsible for the observed viscosity trends.

Here, we rule out other possible explanations of the trends. One could speculate that the difference in mass is responsible for the observed difference in viscosity, but there are several reasons to surmise that this is not actually the case. The mass of the two most abundant components in both solutions, water and chloride, is the same. The cation is the least abundant component, and the mass of Fe is only 2.5 times larger than that of Mg.

Furthermore, we approximate the FeCl₂ and MgCl₂ solutions as effective Lennard-Jones systems, for the sake of a qualitative argument that further illustrates our point. Meier and coworkers^{S35} have shown that, in a Lennard-Jones (LJ) system, the KK and KU integrals are much smaller than the UU integral [see Eqs. (S1) and (S2)], which is the main contribution. For such an LJ system, the viscosity, in reduced units, is universal (i.e., it does not depend on the masses) and it is given in units of $\eta^* = \eta \sigma^2 / \sqrt{m \epsilon}$. In other words, for two systems with the same LJ parameters, the value of the viscosity is proportional to \sqrt{m} . The average mass of a particle (performing the average over molecules of water, cations and anions) in the 4 m FeCl₂ solution is 22.32 g/mol, whereas in the MgCl₂ solution it is 20.46 g/mol. Thus, one would expect the viscosity of the FeCl₂ solution to be about $\sqrt{22.32/20.46} = 1.05$ (i.e., 5% larger) than that of MgCl₂. However, in the experiments, the viscosity of FeCl₂ is 12% lower than that of MgCl₂, resulting in a deviation from the expected result of about 17%. Consequently, we conclude that the mass is not responsible for the observed differences in experimental viscosity at high concentrations. Moreover, we believe that the overestimation of viscosity obtained from our simulations for both MgCl₂ and FeCl₂ is not explained by a known tendency of the Madrid-2019 model to overestimate viscosity (see Sec. S9 for more details).

S7 Predictions of speciation from chemical equilibrium models

A popular (and free) program is Visual MINTEQ,^{S36} that enables the estimation of the population of complexes at 4 m for FeCl₂ and MgCl₂. This program uses the association constants (at infinite dilution) recommended by NIST, and obtains the equilibrium population after solving the equation of balance of mass, charge, iteratively, until all equilibrium constants and user-defined constraints (the concentration, pH, etc) are satisfied. In principle, this seems like a reasonably sound strategy, but these calculations can be sensitive to 1) the association constants, and 2) the activity model used, such as the Specific Ion Theory^{S37–S39} (SIT), Davies equation^{S40}, etc. As detailed in the main text, experiments differ widely in the estimation of association constants.

The program clearly predicts complex formation in both MgCl₂ and FeCl₂ solutions. We emphasize that the quantitative complex populations predicted depend strongly on the chosen activity model. However, independent of the activity model, Visual MINTEQ predicts higher association in MgCl₂ compared to FeCl₂, which goes against the expectation of less complex formation in MgCl₂.^{S41–S43}

S8 Densities from simulations

S8.1 Simulations without complexes

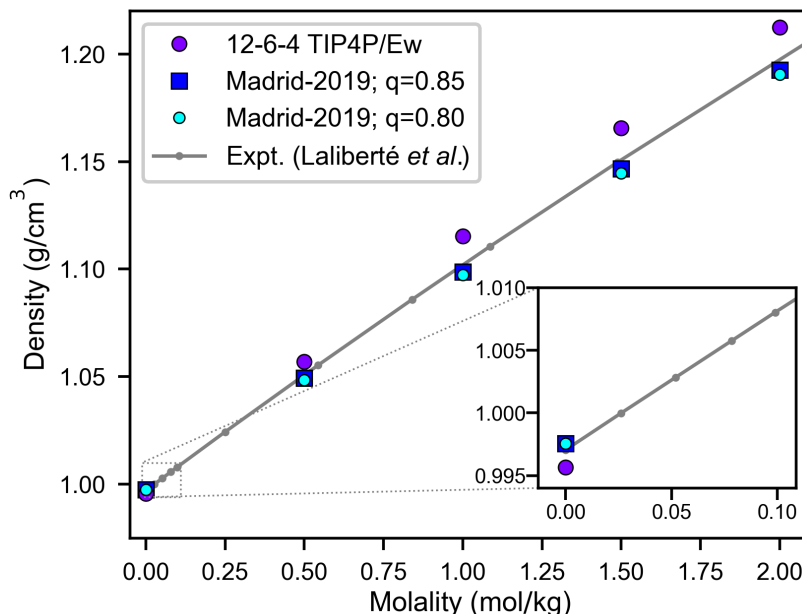


Figure S4: Densities of FeCl_2 obtained from simulations, for low concentrations up to 2 m, using the proposed Madrid-2019^{S1} force-field for FeCl_2 (assuming free ions), and the 12-6-4 potential model of Ref.^{S44} for Fe^{2+} and TIP4P-Ew water along with with the Joung-Cheatham parameters^{S45} for chloride-water interactions (again for TIP4P-Ew). Unlike the Madrid-2019 force field, cross-interactions are obtained using the Lorentz-Berthelot rules for the 12-6-4 potential. Experimental densities in black are taken from Laliberté and Cooper^{S20}. The inset depicts a close-up view of the data for very low molalities, with different ranges on both axes. The Madrid model with $q = 0.80 e$ (cyan circles) uses the same parameters as those of the Madrid-2019 ($q = 0.85 e$) except for the values of σ for the $\text{Cl}-\text{O}_w$ and $\text{Mg}-\text{O}_w$ interactions which are slightly different.

In Fig. S4, we present the results for the density of FeCl_2 , obtained from simulations using the proposed Madrid-2019 force-field, for low concentrations up to 2 m, where complexes are not expected to form. We provide a comparison with a previously published model for Fe^{2+} and water as described by the TIP4P/Ew^{S46} model, the 12-6-4 potential of Li and Merz Jr.^{S44}, using Joung-Cheatham parameters^{S45} for the chloride – water interactions (chloride parameters specifically designed for TIP4P-Ew), and Lorentz-Berthelot mixing rules for cross-interactions. The densities obtained with the 12-6-4 potential show a systematic positive deviation of about 2% from the experimental densities, for concentrations up to 2 m. The agreement of the TIP4P/Ew^{S46} and TIP4P/2005^{S47} water models with experimental data for the density of pure water (i.e., at zero molality) is excellent, with deviations within 0.15%, as shown in the inset. It should be mentioned that the force-field for Fe^{2+} from Ref.^{S44} was designed for the cation at infinite dilution and was not tested at high concentrations of salt.

S8.2 Simulations incorporating complexes

In this work, we also study the effect of complex speciation on the densities. We define α , α' and α'' as the percentage of free cations, monomers and dimers, respectively. Considering a mixture composed of only free cations and monomers, we compare the values of densities for a particular concentration (4 m)

Table S3: Densities (ρ), in g/cm^3 at 298.15 K and 1 bar, of FeCl_2 and MgCl_2 at 4 m, but with varying α (percentage of free cations in the system), calculated using the Madrid-2019 force field for both Fe^{2+} and Mg^{2+} . Note that $\alpha + \alpha' = 100$, since we assume that cations are either free or that they participate in monomers.

System	α	α'	ρ
MgCl_2	100	0	1.248
MgCl_2	15	85	1.254
MgCl_2	2.5	97.5	1.255
FeCl_2	100	0	1.363
FeCl_2	15	85	1.369
FeCl_2	2.5	97.5	1.370

for both MgCl_2 and FeCl_2 , as shown in Table S3. We conclude that the densities are relatively insensitive to complex formation, since the differences in densities correspond to a difference of about 0.5%. We speculate that the density change caused by the inclusion of chloride ions in octahedral solvation shells (compared to a situation in which only water is in an octahedral solvation shell) is not significant.

S9 Overestimation of viscosities by Madrid-2019

The Madrid-2019 model has been known to slightly overestimate viscosities. However, we show that this overestimation cannot explain the large deviation from experimental viscosities for MgCl_2 and FeCl_2 . For instance, in the case of NaCl , the error in the prediction, at 4 m, was ≈ 0.4 mPa·s, whereas for MgCl_2 it is ≈ 2.5 mPa·s. In the same vein, we observe that in the case of $\text{Mg}(\text{ClO}_4)_2$ (a solution which is somewhat similar to MgCl_2) shown in Fig. S5(b), the model overestimates the viscosity by about 1 mPa·s.

We argue that complex formation in FeCl_2 and MgCl_2 solutions, at higher concentrations, causes the deviations in computed viscosities (from simulations wherein all cations are free). Artificially inserting complexes (such that all cations form "dimers" or $[\text{Mg}(\text{H}_2\text{O})_4\text{Cl}_2]$ complexes) brings the computed viscosity value closer to the experimental value, as shown in Fig. S5.

S10 Speciation effects on transport properties

Table S4: Viscosity (in mPa·s) of FeCl_2 and MgCl_2 solutions at 4 m obtained from simulations. α denotes the percentage of free cations in the system (only monomers are considered so that $\alpha + \alpha' = 100$). The Yeh-Hummer correction^{S7} is applied to the diffusion coefficients to account for finite-size effects.

System	α	$D_{\text{H}_2\text{O}} \times 10^9$ (m^2/s)	η (mPa·s)
MgCl_2	100	0.366	7.73(0.39)
MgCl_2	15	0.499	5.71(0.33)
MgCl_2	2.5	0.522	5.56(0.42)
FeCl_2	100	0.369	7.68(0.41)
FeCl_2	15	0.496	5.87(0.30)
FeCl_2	2.5	0.522	5.54(0.32)

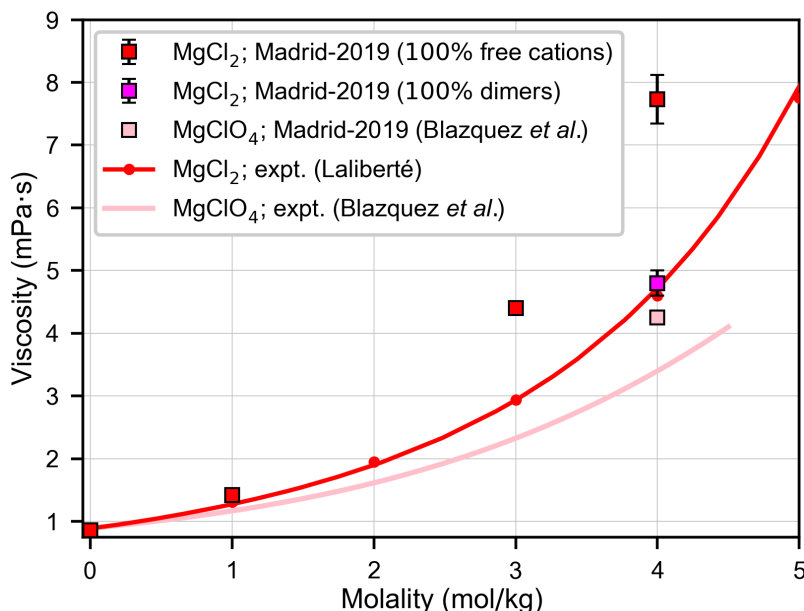


Figure S5: Viscosities of MgCl_2 (solid red line) and $\text{Mg}(\text{ClO}_4)_2$ from experiments (solid pink line) and from simulations with the Madrid-2019 force-field (filled red and pink squares, respectively). Simulation results at 4 m are from this work. Experimental results for $\text{Mg}(\text{ClO}_4)_2$ are from Blazquez et al.^{S3} Filled magenta square: simulation results for the Madrid-2019 force field of MgCl_2 at 4 m assuming that all cations form $[\text{Mg}(\text{H}_2\text{O})_4\text{Cl}_2]$.

The viscosity and diffusion coefficient obtained in simulations for 4 m solutions of FeCl_2 and MgCl_2 are presented in Table S4.

Table S5: The product of the diffusion coefficient of water, and the viscosity of the solution ($D_{\text{H}_2\text{O}} \times \eta$), reported in units of $10^{12} \times \text{J/m}$, for FeCl_2 and MgCl_2 at 4 m. α denotes the percentage of free cations in the system. The Yeh-Hummer correction^{S7} was applied to the diffusion coefficients (shown in units of m^2/s after being multiplied by 10^9) to account for finite-size effects. Note that $\alpha + \alpha' = 100$, since we assume that cations are either free or that they participate in monomers.

System	α	$D_{\text{H}_2\text{O}} \times \eta$
MgCl_2	100	2.8
MgCl_2	15	2.8
MgCl_2	2.5	2.9
FeCl_2	100	2.8
FeCl_2	15	2.9
FeCl_2	2.5	2.9

In Table S5, we present the product of the $D_{\text{H}_2\text{O}}$ and the viscosity of the system. This product is approximately constant and it is around $2.8(2) \cdot 10^{12} \text{ J/m}$. This is interesting, since it shows that a rough estimate of the viscosity can be obtained from the diffusion coefficient of water (a relatively cheap calculation).

The diffusion of the cations is shown in Table S6. For $\alpha = 100$, the diffusion of Fe is smaller than that of Mg (as expected from its higher mass). When monomers are formed, the diffusion coefficient of the cation increases significantly both for the free cation and for the cation forming the complex.

Table S6: Diffusion coefficient ($\times 10^9 \text{m}^2/\text{s}$) of the cations of FeCl_2 and MgCl_2 at 4 m using the same force field for Fe^{2+} and Mg^{2+} . Results are shown for $\alpha = 100$ (free ions, no monomers) and for $\alpha = 2.5$ (the majority of the cations is in the monomer form). Note that $\alpha + \alpha' = 100$, since we assume that cations are either free or that they participate in monomers.

	$\alpha = 100$	$\alpha = 2.5$
	$D_{\text{M}^{2+}}$	$D_{\text{M}^{2+}}, D_{\text{MCl}^+}$
MgCl_2	0.0955	0.15(5), 0.129(4)
FeCl_2	0.0922	0.15(3), 0.130(2)

S11 Back-of-the-envelope calculation for viscosities

Table S7: Changes in the viscosity η in $\text{mPa}\cdot\text{s}$, of MgCl_2 at the concentration of 4 m with the degree of association. Calculations are performed with the Madrid-2019 force field using the $q = 0.8 e$ model. Results are presented for free ions $\alpha = 100$, monomers $\alpha' = 100$ and dimers $\alpha'' = 100$

System	α	α'	α''	η
Free ion	100	0	0	5.33(0.3)
monomer complexes	0	100	0	4.12(0.3)
dimer complexes	0	0	100	3.90(0.3)

In the main text, we proposed a simple relation between the viscosity with 100% free ions, and the distribution of complexes (α , α' and α'')

Here, we estimate the coefficients of α' and α'' in Eq (2) in the main text, denoted by δ' and δ'' , respectively (the rate of change of viscosity with α'' or α'). Therefore, for the $q = 0.85 e$ and $q = 0.80 e$ Madrid-2019 models, we obtain $\delta' = 0.020 \text{ mPa}\cdot\text{s}$ and $\delta'' = 0.010 \text{ mPa}\cdot\text{s}$, respectively, from the slopes of lines fitted to the data in Fig. 3 of the main text.

The value of δ'' for the $q = 0.85 e$ model can be obtained from:

$$\begin{aligned} & \frac{\eta_{(\alpha=100, \alpha'=0, \alpha''=0)} - \eta_{(\alpha=0, \alpha'=0, \alpha''=100)}}{100} \\ &= \frac{7.73 - 4.80}{100} \text{ mPa}\cdot\text{s} \\ &\approx 0.029 \text{ mPa}\cdot\text{s}, \end{aligned} \quad (\text{S3})$$

where the viscosity values were obtained for the $q = 0.85$ Madrid-2019 model.

The value of δ'' for the $q = 0.8 e$ model can be obtained from:

$$\begin{aligned} & \frac{\eta_{(\alpha=100, \alpha'=0, \alpha''=0)} - \eta_{(\alpha=0, \alpha'=0, \alpha''=100)}}{100} \\ &= \frac{5.33 - 3.90}{100} \text{ mPa}\cdot\text{s} \\ &\approx 0.014 \text{ mPa}\cdot\text{s}, \end{aligned} \quad (\text{S4})$$

where the viscosity values were obtained for the $q = 0.8 e$ Madrid-2019 model, collected in Table S7.

Furthermore, we provide justifications for the values taken for $\log K_1$ and $\log K_2$. Values of $\log K_1$ (i.e., logarithm to base 10) and $\log K_2$ for some divalent cations with many ligands can be found in the monumental and trusted Lange's Handbook.^{S48} For Fe^{2+} , the handbook only reports $\log K_1$ and refers

to the value of Martell and Smith^{S49} (equal to 0.36). However, the handbook does provide the values of $\log K_1$ and $\log K_2$ for Fe^{3+} , equal to 1.48 and 0.65, respectively, as well as those for Pb^{2+} , equal to 1.62 and 0.82, respectively. Of course, the individual values depend on the cation, but we observe that the approximation $\log K_2 \approx \log K_1 - 0.8$ seems reasonable. Intuitively, this makes sense since the Cl^- - Cl^- electrostatic repulsion would make the formation of the second complex somewhat less favorable (that means that the second equilibrium constant is similar to the first and differs from it, at most, by an order of magnitude). In this experiment, we shall set all activity coefficients to 1 (we stress, once again, that we are just attempting to do a qualitative calculation). By assuming the value -0.20 for $\log K_1$ from NIST, and -1.0 for $\log K_2$, we obtain (for a 4 m solution of FeCl_2): $\alpha = 22$, $\alpha' = 56$ and $\alpha'' = 22$ (Visual MINTEQ with the SIT model, and without dimer formation included, would lead to $\alpha = 29$, which is not so different from our value). By replacing the value η^0 for the model with $q = 0.8$ (i.e 5.33 mPa·s for $\alpha = 100$), and using Eq. (6) from the main text with these values of α , α' and α'' , one obtains 4.46 mPa·s for the viscosity of FeCl_2 , which is not so different from the experimental value measured in this work (equal to 4.17 mPa·s; see Table 1 in the main text). By assuming a $\log K_1$ of -1.1 for MgCl_2 (i.e., 0.9 below the value of FeCl_2), and $\log K_2 = -1.1 - 0.8 = -1.9$ we obtain, for a 4 m solution of MgCl_2 : $\alpha = 64$, $\alpha' = 33$, $\alpha'' = 3$. Similarly, we obtain 4.96 mPa·s for the viscosity of MgCl_2 , which is very close to the viscosity of MgCl_2 from experiments (as shown in Fig. S1).

S12 Evaluation of the Jones-Dole coefficient of a force-field

The Jones-Dole equation describes the variation of the viscosity of electrolyte solutions quite well, according to the relation:

$$\eta/\eta_w = 1 + A\sqrt{m} + Bm + Cm^2 + \dots \quad (\text{S5})$$

where η is the viscosity of the solution at molality m and η_w is the viscosity of pure water. The coefficient A is always positive and rather small and is at least one order of magnitude smaller than B . The term A captures the viscosity change due to Coulombic ion-ion interactions. The term B originates from from ion-water interactions, and the term C represents the interactions between hydrated ions and the formation of complexes. Determining A and B from simulations is a *tour of force*, as it requires extremely long simulations to estimate the viscosity with very high accuracy at low concentrations. In fact, there is only one paper in the literature^{S50} which rigorously evaluates the Jones-Dole coefficients for certain popular force-fields of 1:1 electrolytes. In that work, B coefficients were obtained by fitting the simulation results for concentrations between 0.1 and 1 m, while the values of A were not reported, since the associated statistical error was larger than the absolute values. In this work, we estimate the B coefficients by using the simple expression (obtained from Eq. (S5) after neglecting the quadratic term):

$$B' \simeq (\eta/\eta_w - 1 - A\sqrt{m})/m \quad (\text{S6})$$

Given that $A \ll B$, we use the experimental values of A to obtain B' . The value of A is ≈ 0.02 (kg/mol)^{1/2} for 2:1 electrolytes^{S51}. Furthermore, the results of Yue and Panagiotopoulos^{S50} strongly suggest that the values of A of atomistic force-fields are very close to the experimental ones. To evaluate B' , a concentration which is low enough that the quadratic term contribution in the Jones-Dole equation (Eq. (S5)) can be neglected is needed. We shall use 0.6 m for MgCl_2 and FeCl_2 . In fact, if one uses experimental results^{S19} for η and η_w at 0.6 m for CaCl_2 and MgCl_2 in Eq. (S6), one obtains a value of B' that is only 0.01 kg/mol higher than the experimental value of B reported by Marcus^{S51,S52} for these salts (0.01 kg/mol is also the experimental uncertainty of B). The notation B' just reflects that B' (as given by Eq. (S6)) is an approximation of the true value of B (although it is a good approximation as when implemented with experimental values of viscosities since it deviates by only 0.01 kg/mol from the exact value of B).

In order to determine the coefficient B' , we performed 24 independent simulations (at 0.6 m) in the NVT ensemble (keeping the rest of the simulation details the same as those specified in Sec. S1.1) of 20 ns each (i.e., we used a total simulation time of 480 ns to determine the viscosity of one salt and force-field). The volume used in the NVT simulations was obtained from a NpT run of 20 ns. The system contains 4440 molecules of water and the number of ions needed for the required concentration, i.e., 0.6 m. Our estimated uncertainty for B' is 0.03 kg/mol (obtained from the uncertainties of the viscosities of the solutions and that of pure water plus that introduced by Eq. (S6)). The viscosity of TIP4P/2005 water at 298.15 K and 1 bar is 0.866(3) mPa·s (the experimental one is 0.890 mPa·s). Using the force-field described in the main text for the scaled charge 0.8, we obtained (at 0.6 m and 298.15 K and 1 bar) a viscosity of 1.120(4) mPa·s for FeCl_2 and of 1.097(4) for MgCl_2 . Therefore, we obtained $B' = 0.46(3)$ kg/mol for FeCl_2 and $B' = 0.42(3)$ kg/mol for MgCl_2 .

References

- S1. Zeron, I.; Abascal, J.; Vega, C. A force field of Li^+ , Na^+ , K^+ , Mg^{2+} , Ca^{2+} , Cl^- , and SO_4^{2-} in aqueous solution based on the TIP4P/2005 water model and scaled charges for the ions. *J. Chem. Phys.* **2019**, *151*, 134504.
- S2. Abascal, J. L. F.; Vega, C. A general purpose model for the condensed phases of water: TIP4P/2005. *J. Chem. Phys.* **2005**, *123*, 234505.
- S3. Blazquez, S.; Troncoso, J.; La Francesca, P.; Gallo, P.; Conde, M.; Vega, C. Extending the Madrid-2019 force field to the perchlorate anion: role of charge distribution and validation with experiments on Mars-relevant aqueous solutions. *J. Mol. Liq.* **2025**, *435*, 128035.
- S4. Blazquez, S.; Conde, M.; Vega, C. Scaled charges for ions: An improvement but not the final word for modeling electrolytes in water. *J. Chem. Phys.* **2023**, *158*, 054505.
- S5. Abraham, M. J.; Murtola, T.; Schulz, R.; Páll, S.; Smith, J. C.; Hess, B.; Lindahl, E. GROMACS: High performance molecular simulations through multi-level parallelism from laptops to supercomputers. *SoftwareX* **2015**, *1–2*, 19–25.
- S6. Thompson, A. P.; Aktulga, H. M.; Berger, R.; Bolintineanu, D. S.; Brown, W. M.; Crozier, P. S.; in 't Veld, P. J. I.; Kohlmeyer, A.; Moore, S. G.; Nguyen, T. D.; Shan, R.; Stevens, M. J.; Tranchida, J.; Trott, C.; Plimpton, S. J. LAMMPS - a flexible simulation tool for particle-based materials modeling at the atomic, meso, and continuum scales. *Comput. Phys. Commun.* **2022**, *271*, 108171.
- S7. Yeh, I.; Hummer, G. System-size dependence of diffusion coefficients and viscosities from molecular dynamics simulations with periodic boundary conditions. *J. Phys. Chem. B* **2004**, *108*, 15873–15879.
- S8. Evans, D. J.; Holian, B. L. The Nose–Hoover thermostat. *J. Chem. Phys.* **1985**, *83*, 4069–4074.
- S9. Parrinello, M.; Rahman, A. Polymorphic transitions in single crystals: A new molecular dynamics method. *J. Appl. Phys.* **1981**, *52*, 7182–7190.
- S10. Nosé, S.; Klein, M. Constant pressure molecular dynamics for molecular systems. *Mol. Phys.* **1983**, *50*, 1055–1076.
- S11. Hess, B.; Bekker, H.; Berendsen, H. J.; Fraaije, J. G. LINCS: A linear constraint solver for molecular simulations. *J. Comput. Chem.* **1997**, *18*, 1463–1472.

- S12. Shinoda, W.; Shiga, M.; Mikami, M. Rapid estimation of elastic constants by molecular dynamics simulation under constant stress. *Phys. Rev. B* **2004**, *69*, 134103.
- S13. Hockney, R. W.; Eastwood, J. W. *Computer simulation using particles*; CRC Press: Boca Raton, 2021.
- S14. Ryckaert, J.-P.; Ciccotti, G.; Berendsen, H. J. Numerical integration of the cartesian equations of motion of a system with constraints: molecular dynamics of n-alkanes. *J. Comput. Phys.* **1977**, *23*, 327–341.
- S15. Martínez, L.; Andrade, R.; Birgin, E. G.; Martínez, J. M. PACKMOL: A package for building initial configurations for molecular dynamics simulations. *J. Comput. Chem.* **2009**, *30*, 2157–2164.
- S16. Jewett, A. I.; Stelter, D.; Lambert, J.; Saladi, S. M.; Roscioni, O. M.; Ricci, M.; Autin, L.; Maritan, M.; Bashusqeh, S. M.; Keyes, T.; Dame, R. T.; Shea, J.-E.; Jensen, G. J.; Goodsell, D. S. Moltemplate: A Tool for Coarse-Grained Modeling of Complex Biological Matter and Soft Condensed Matter Physics. *J. Mol. Biol.* **2021**, *433*, 166841.
- S17. Hjorth Larsen, A. et al. The atomic simulation environment—a Python library for working with atoms. *J. Phys. Condens. Matter* **2017**, *29*, 273002.
- S18. Gonzalez, M. A.; Abascal, J. L. F. The shear viscosity of rigid water models. *J. Chem. Phys.* **2010**, *132*, 096101.
- S19. Laliberté, M. Model for calculating the viscosity of aqueous solutions. *J. Chem. Eng. Data* **2007**, *52*, 321–335.
- S20. Laliberté, M.; Cooper, W. E. Model for calculating the density of aqueous electrolyte solutions. *J. Chem. Eng. Data* **2004**, *49*, 1141–1151.
- S21. Königsberger, E.; Königsberger, L.-C.; Szilágyi, I.; May, P. M. Measurement and Prediction of Physicochemical Properties of Liquors Relevant to the Sulfate Process for Titania Production. 1. Densities in the $\text{TiOSO}_4 + \text{FeSO}_4 + \text{H}_2\text{SO}_4 + \text{H}_2\text{O}$ System. *J. Chem. Eng. Data* **2008**, *54*, 520–525.
- S22. Uroš Luin, U.; Arcon, I.; Valant, M. Structure and population of complex ionic species in FeCl_2 aqueous solution by X-ray absorption spectroscopy. *Molecules* **2022**, *27*, 642.
- S23. Ohtaki, H.; Radnai, T. Structure and dynamics of hydrated ions. *Chem. Rev.* **1993**, *93*, 1157–1204.
- S24. Marcus, Y. Ionic radii in aqueous solutions. *Chem. Rev.* **1988**, *88*, 1475–1498.
- S25. Marcus, Y. Thermodynamics of solvation of ions. Part 5.—Gibbs free energy of hydration at 298.15 K. *J. Chem. Soc. Faraday Trans.* **1991**, *87*, 2995–2999.
- S26. Persson, I. Hydrated metal ions in aqueous solution: How regular are their structures? *Pure Appl. Chem.* **2010**, *82*, 1901–1917.
- S27. Zapałowski, M.; Bartczak, W. M. Concentrated aqueous MgCl_2 solutions. A Computer simulation study of the solution structure and excess electron localisation. *Res. Chem. Intermed.* **2001**, *27*, 855–866.
- S28. Schmidt, H.; Hennings, E.; Voigt, W. Magnesium chloride tetrahydrate, $\text{MgCl}_2 \cdot 4\text{H}_2\text{O}$. *Acta Crystallogr. C* **2011**, *68*, i4–i6.

- S29. Lind, M. D. Crystal Structure of Ferric Chloride Hexahydrate. *J. Chem. Phys* **1967**, *47*, 990–993.
- S30. Kuppuraj, G.; Dudev, M.; Lim, C. Factors governing metal- ligand distances and coordination geometries of metal complexes. *J. Phys. Chem. B* **2009**, *113*, 2952–2960.
- S31. Wei, Z.; Xu, H.; Xu, X.; Feng, G.; Zheng, W.; Li, T. Solvation of magnesium chloride dimer in water: The case of anionic and neutral clusters. *J. Chem. Phys* **2023**, *158*, 174311.
- S32. Wróbel, P.; Kubisiak, P.; Eilmes, A. Quantum-Chemical and Molecular Dynamics Investigations of Magnesium Chloride Complexes in Dimethoxyethane Solutions. *ACS Omega* **2020**, *5*, 12842–12852.
- S33. Shi, R.; Cooper, A. J.; Tanaka, H. Impact of hierarchical water dipole orderings on the dynamics of aqueous salt solutions. *Nat. Commun* **2023**, *14*, 4616.
- S34. Chaudhari, M. I.; Vanegas, J. M.; Pratt, L.; Muralidharan, A.; Rempe, S. B. Hydration mimicry by membrane ion channels. *Annu. Rev. Phys. Chem* **2020**, *71*, 461–484.
- S35. Karsten Meier, K.; Laesecke, A.; Kabelac, S. Transport coefficients of the Lennard-Jones model fluid. I Viscosity. *J. Chem. Phys* **2004**, *121*, 3671.
- S36. Gustafsson, J. P. Visual MINTEQ 3.0 user guide. *KTH, Department of Land and Water Resources, Stockholm, Sweden* **2011**, 550.
- S37. Bronsted, J. N. Studies on solubility IV. The principle of the specific interaction of ions. *J. Am. Chem. Soc.* **1922**, *44*, 877.
- S38. Guggenheim, E.; Turgeon, J. Specific interaction of ions. *Trans. Faraday Soc.* **1955**, *51*, 747.
- S39. Ciavatta, L. The specific interaction theory in the evaluating ionic equilibria. *Trans. Faraday Soc.* **1980**, *70*, 551.
- S40. Davies, C. W. 397. The extent of dissociation of salts in water. Part VIII. An equation for the mean ionic activity coefficient of an electrolyte in water, and a revision of the dissociation constants of some sulphates. *J. Chem. Soc.* **1938**, *8*, 2093.
- S41. Duboué-Dijon, E.; Mason, P. E.; Fischer, H. E.; Jungwirth, P. Hydration and ion pairing in aqueous Mg²⁺ and Zn²⁺ solutions: Force-field description aided by neutron scattering experiments and ab initio molecular dynamics simulations. *J. Phys. Chem. B* **2017**, *122*, 3296–3306.
- S42. Böhm, F.; Sharma, V.; Schwaab, G.; Havenith, M. The low frequency modes of solvated ions and ion pairs in aqueous electrolyte solutions: iron(II) and iron(III) chloride. *Phys. Chem. Chem. Phys* **2015**, *17*, 19582–19591.
- S43. Luin, U.; Arçon, I.; Valant, M. Structure and population of complex ionic species in FeCl₂ aqueous solution by X-ray absorption spectroscopy. *Molecules* **2022**, *27*, 642.
- S44. Li, P.; Merz Jr, K. M. Taking into account the ion-induced dipole interaction in the nonbonded model of ions. *J. Chem. Theory Comput.* **2014**, *10*, 289–297.
- S45. Joung, I. S.; Cheatham III, T. E. Determination of alkali and halide monovalent ion parameters for use in explicitly solvated biomolecular simulations. *J. Phys. Chem. B* **2008**, *112*, 9020–9041.

- S46. Horn, H. W.; Swope, W. C.; Pitara, J. W.; Madura, J. D.; Dick, T. J.; Hura, G. L.; Head-Gordon, T. Development of an improved four-site water model for biomolecular simulations: TIP4P-Ew. *J. Chem. Phys* **2004**, *120*, 9665–9678.
- S47. Abascal, J. L. F.; Vega, C. A general purpose model for the condensed phases of water: TIP4P/2005. *J. Chem. Phys* **2005**, *123*, 234505.
- S48. Dean, J. A. *Lange's Handbook of Chemistry, 15th Edition*; McGraw-Hill: New York, 1999.
- S49. Martell, A. E.; Smith, R. M. *Critical stability constants*; Springer, 1974; Vol. 1.
- S50. Yue, S.; Panagiotopoulos, A. Z. Dynamic properties of aqueous electrolyte solutions from non-polarisable, polarisable, and scaled-charge models. *Mol. Phys.* **2019**, *117*, 3538–3549.
- S51. Jenkins, H. D. B.; Marcus, Y. Viscosity B-Coefficients of Ions in Solution. *Chem. Rev.* **1995**, *95*, 2695.
- S52. Marcus, Y. *Ion Properties*; Marcel Dekker, Inc., 1997.

TOC Graphic

